3

Orbit dynamics and trajectory elements

In this chapter the basic equations for the calculation of orbits and trajectories are given, and the properties of the most important types of trajectories used in rendezvous missions are discussed. In sections 3.1 and 3.2 the reference frames are defined and the laws of motion in elliptic and circular orbits in the 'orbital plane' coordinate frame are addressed. Equations of motion, expressed in this frame, are conveniently used during launch and phasing operations. In sections 3.3 and 3.4, the trajectories between chaser and target vehicle which are used in the far and close range rendezvous approaches are discussed. They are treated as relative trajectories in the 'local orbital frame' of the target. Only the ideal undisturbed trajectories are looked at in this chapter, and the necessary velocity changes, or continuous forces to be applied and the resulting position changes, are derived for ideal cases. The major sources of trajectory disturbances are addressed in chapter 4.

3.1 Reference frames

The purpose of this section is to define the coordinate frames used in this book for the description of the orbital motion, for absolute and relative trajectory and attitude motions and for the relations of these motions to geometric features on the spacecraft. Each frame $\mathbf{F}_i$ is defined by its origin $\mathbf{O}_i$ and a set of three orthogonal vectors $\mathbf{a}_1, \mathbf{a}_2, \mathbf{a}_3$. Generally three types of coordinate frames are needed:

- *Orbit reference frames:* to describe the orientation of the orbit relative to inertial space and to the Earth and to describe the motion of a spacecraft within an orbit.
- *Spacecraft local orbital reference frames:* to describe the motion relative to a particular point in orbit or to another spacecraft.

- *Spacecraft attitude and body frames:* to describe dynamic and kinematic processes (attitude, attitude manoeuvres) of the spacecraft relative to its centre of mass and to describe features relative to the geometry and to a particular point of the spacecraft.

3.1.1 Earth-centred equatorial frame F_{eq}

The F_{eq} coordinate frame will be used to describe the orbital motion around the centre of the Earth and w.r.t. inertially fixed directions. The Earth is assumed to be truly spherical, i.e. its geometric centre is its centre of mass and the focal point of orbital motions.

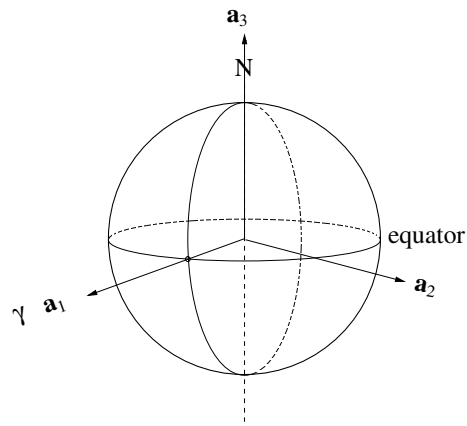

Figure 3.1. F_{eq} frame.

In figure 3.1 we have:

- origin $\mathbf{O}_{\mathrm{eq}}$: centre of the Earth;
- axis $\mathbf{a}_1$: in the equatorial plane, pointing toward the mean of the vernal equinox;
- axis $\mathbf{a}_2$: in the equatorial plane, such that $\mathbf{a}_3 = \mathbf{a}_1 \times \mathbf{a}_2$;
- axis $\mathbf{a}_3$: normal to the equatorial plane and pointing north.

$\boldsymbol{F}_{\mathbf{eq}}$ can be used as a quasi-inertial frame.

3.1.2 Orbital plane frame $\boldsymbol{F}_{\mathbf{op}}$

The F_{op} coordinate frame is used when only the motion within the orbital plane has to be described.

In figure 3.2 we have:

- origin $\boldsymbol{O}_{\mathbf{op}}$: centre of the Earth;

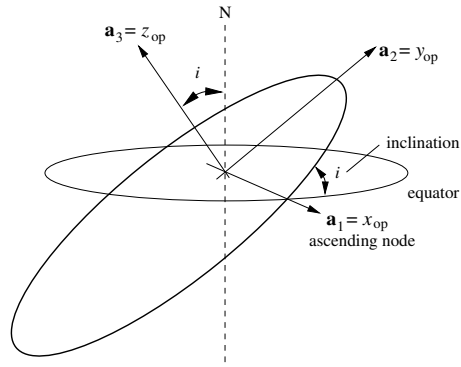

Figure 3.2. F_{op} frame.

- axis $\mathbf{a}_1$: in the orbital plane, pointing toward the ascending node;
- axis $\mathbf{a}_2$: in the orbital plane, such that $\mathbf{a}_3 = \mathbf{a}_1 \times \mathbf{a}_2$;
- axis $\mathbf{a}_3$: normal to orbital plane, inclined to the north direction by the angle i.

The coordinate transformation from the Earth-centred equatorial frame $\boldsymbol{F}_{\mathbf{eq}}$ to the orbital plane frame $\boldsymbol{F}_{\mathbf{op}}$ is obtained by a rotation about z_{eq} by the RAAN angle Ω (see figure 2.3) and by a further rotation about the axis through the nodes by the inclination angle i:

$$\begin{bmatrix} x_{\text{op}} \\ y_{\text{op}} \\ z_{\text{op}} \end{bmatrix} = \begin{bmatrix} 1 & 0 & 0 \\ 0 & \cos i & \sin i \\ 0 & -\sin i & \cos i \end{bmatrix} \begin{bmatrix} \cos\Omega & \sin\Omega & 0 \\ -\sin\Omega & \cos\Omega & 0 \\ 0 & 0 & 1 \end{bmatrix} \begin{bmatrix} x_{\text{eq}} \\ y_{\text{eq}} \\ z_{\text{eq}} \end{bmatrix}$$

$\boldsymbol{F}_{\mathbf{op}}$ can be used to describe orbital transfer manoeuvres.

3.1.3 Spacecraft local orbital frame $\boldsymbol{F}_{\mathbf{lo}}$

The F_{lo} coordinate frame is used to describe motions w.r.t. the moving position and direction towards the centre of the Earth of an orbiting body.

In figure 3.3 we have:

- origin $\boldsymbol{O}_{\mathbf{lo}}$: centre of mass of the spacecraft;
- axis $\mathbf{a}_1$: $\mathbf{a}_1 = \mathbf{a}_2 \times \mathbf{a}_3$ ($\mathbf{a}_1$ is in the direction of the orbital velocity vector but not necessarily aligned with it). In the rendezvous literature this coordinate is also called **V-bar**;
- axis $\mathbf{a}_2$: in the opposite direction of the angular momentum vector of the orbit. In the rendezvous literature this coordinate is also called **H-bar**;

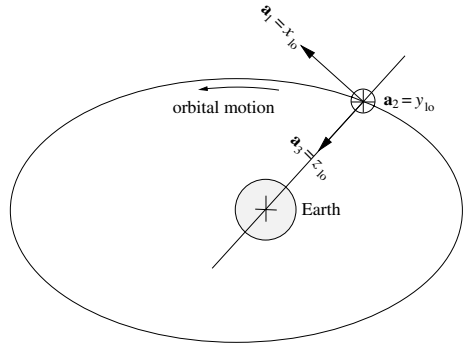

Figure 3.3. F_{lo} frame.

- axis $\mathbf{a}_3$: radial from the spacecraft CoM to the centre of the Earth.
  In the rendezvous literature this coordinate is also called **R-bar**.

In this way the local orbital frame for both the target and the chaser can be defined. The approach trajectories of the chaser are usually shown in the local orbital frame of the target. This frame is often referred to as the local-vertical/local-horizontal (LVLH) frame.

The coordinate transformation from the orbital plane frame $\boldsymbol{F}_{\mathbf{op}}$ to the spacecraft local orbital frame $\boldsymbol{F}_{\mathbf{lo}}$ is obtained by a rotation about z_{op} by the orbital phase angle ϕ, measured from the ascending node, and by two 90 deg rotations to put x_{lo} into the orbital velocity direction and z_{lo} toward the centre of the Earth. For a circular orbit $\phi = \omega\, t$. For near circular orbits, as used in most rendezvous missions, this is a good approximation:

$$\begin{bmatrix} x_{\mathrm{lo}} \\ y_{\mathrm{lo}} \\ z_{\mathrm{lo}} \end{bmatrix} = \begin{bmatrix} 1 & 0 & 0 \\ 0 & 0 & -1 \\ 0 & 1 & 0 \end{bmatrix} \begin{bmatrix} 0 & 1 & 0 \\ -1 & 0 & 0 \\ 0 & 0 & 1 \end{bmatrix} \begin{bmatrix} \cos\phi & \sin\phi & 0 \\ -\sin\phi & \cos\phi & 0 \\ 0 & 0 & 1 \end{bmatrix} \begin{bmatrix} x_{\mathrm{op}} \\ y_{\mathrm{op}} \\ z_{\mathrm{op}} \end{bmatrix}$$

3.1.4 Spacecraft attitude frame $\boldsymbol{F}_{\mathbf{a}}$

The spacecraft attitude frame is used to describe all rotations of the body of a spacecraft. The attitude frame is often referred to as the 'body frame'. However, as the CoM may move during flight, e.g. due to depletion of propellant, this frame is not firmly fixed to the spacecraft geometry.

The nominal direction of the spacecraft attitude frame depends on the manoeuvre strategy of the mission. The axis $\mathbf{a}_1$ may point in the direction of the orbital velocity vector, toward the Earth, the Sun or in other directions. For example, in the final phase of a rendezvous and docking mission, the axis $\mathbf{a}_1$ is usually pointing in the direction of the docking axis. The lateral axis $\mathbf{a}_2$ is often aligned with the positive or negative direction of the angular momentum vector of the orbit. In figure 3.4 we have

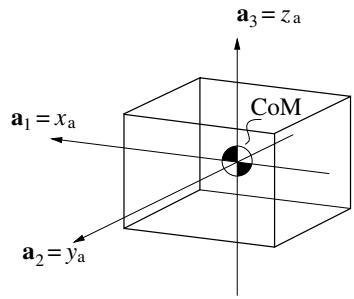

Figure 3.4.

- origin $\boldsymbol{O}_\mathbf{a}$: centre of mass of the spacecraft;
- direction of axes $\mathbf{a}_1, \mathbf{a}_2, \mathbf{a}_3$ depending on mission and mission phase, $\mathbf{a}_3 = \mathbf{a}_1 \times \mathbf{a}_2$ forming a right handed system.

The coordinate transformation from the LVLH frame $\boldsymbol{F}_\mathbf{lo}$ to the spacecraft nominal attitude frame $\boldsymbol{F}_\mathbf{a}$ is obtained by a rotation of the frame by the attitude angles α_z (azimuth), α_y (elevation) and α_x (roll):

$$\begin{bmatrix} x_\mathrm{a} \\ y_\mathrm{a} \\ z_\mathrm{a} \end{bmatrix} = \begin{bmatrix} 1 & 0 & 0 \\ 0 & c\alpha_x & s\alpha_x \\ 0 & -s\alpha_x & c\alpha_x \end{bmatrix} \begin{bmatrix} -s\alpha_y & 0 & c\alpha_y \\ 0 & 1 & 0 \\ c\alpha_y & 0 & s\alpha_y \end{bmatrix} \begin{bmatrix} c\alpha_z & s\alpha_z & 0 \\ -s\alpha_z & c\alpha_z & 0 \\ 0 & 0 & 1 \end{bmatrix} \begin{bmatrix} x_\mathrm{lo} \\ y_\mathrm{lo} \\ z_\mathrm{lo} \end{bmatrix}$$

$$s\alpha = \sin\alpha$$
$$c\alpha = \cos\alpha$$

3.1.5 Spacecraft geometric frames $\boldsymbol{F}_\mathbf{ge}$

These coordinate frames are used to describe translations and rotations of the spacecraft w.r.t. location and direction of equipment, such as sensors, thrusters or docking mechanism. In figure 3.5 we have

- origin $\boldsymbol{O}_\mathbf{ge}$: a particular point on the spacecraft, e.g.
  - the point defining the origin of the spacecraft coordinate system,
  - the centre of the docking port, defining the docking frame,
  - the centre of a sensor, defining the measurement frame;
- axes $\mathbf{a}_1, \mathbf{a}_2, \mathbf{a}_3$: coordinate-aligned with, or under a fixed angle to, the attitude frame.

The transformation from the spacecraft attitude frame to one of the geometric frames is a parallel shift in *x*, *y*, *z* from the centre of mass of the spacecraft and a fixed rotation ϕ_x, ϕ_y, ϕ_z around the origin of the frame. It requires, therefore, the knowledge of the instantaneous position of the CoM of the spacecraft.

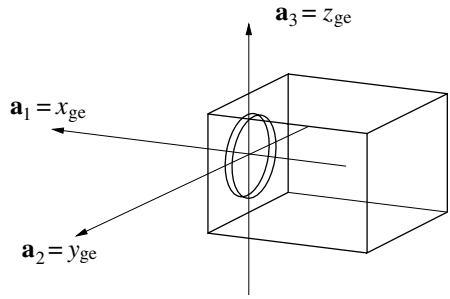

Figure 3.5. F_{ge} frame.

3.2 Orbit dynamics

3.2.1 Orbital motion around a central body

The equations of motion in an orbit around a central body can be derived from Kepler's and Newton's laws. The detailed derivation of these equations is provided in many textbooks, such as Kaplan (1976), Roy (1988), Renner, Nauck & Balteas (1988), Wertz & Larson (1991), Carrou (1995) and Sidi (1997).

To enable the understanding of rendezvous trajectories, only the most important relations will be repeated here; these are valid for the case of an undisturbed spherical gravitational field (relations are given in the orbital plane frame).

Combining Newton's laws of gravitation

$$F = -G\frac{m_c m_s}{r^2} \tag{3.1}$$

with his second law, relating force and acceleration,

$$F = m_s \ddot{r} \tag{3.2}$$

one obtains the equation for the orbital motion of a satellite:

$$\ddot{r} = -\frac{\mu}{r^2} \tag{3.3}$$

In these equations $G = 6.674 \times 10^{-11}\,\mathrm{N\,m^2/kg^2}$ is the universal gravitational constant, m_c is the mass of the central body, m_s is the mass of the satellite and r is the distance between their centres. The term $\mu = G \cdot m_c$ is the gravitational constant of the celestial body around which the satellite orbits. The gravitational constant of the Earth is $\mu_E = 398\,600\,\mathrm{km^3/s^2}$. A solution to Eq. (3.3) is:

$$r = \frac{p}{1 + e\cos\nu} \tag{3.4}$$

with p being a parameter defining the geometric extension of the curve, e the eccentricity and ν the polar angle measured from the pericentre (true anomaly). This is the general equation for conic sections. Derivations can be found in Roy (1988), Renner *et al.* (1988) and Sidi (1997). The value of *e* defines the shape of the curve:

for $e = 0$ the curve is a circle,
for $0 < e < 1$ the curve is an ellipse,
for $e = 1$ the curve is a parabola,
for $e > 1$ the curve is a hyperbola.

Of these four possible conic sections, circle, ellipse, parabola and hyperbola, only the first two are of interest for the discussion of rendezvous trajectories in this book.

Elliptic orbits

In an elliptic orbit, Eq. (3.4) becomes at the apocentre for $\nu = 180$ deg

$$r_{\mathrm{a}} = \frac{p}{1-e}$$

and at the pericentre for $\nu = 0$

$$r_{\mathrm{p}} = \frac{p}{1+e}$$

and with $r_{\mathrm{a}} + r_{\mathrm{p}} = 2a$, the parameter becomes $p = a(1-e^2)$. The polar equation of an elliptic orbit is then

$$r = \frac{a(1-e^2)}{1+e\,\cos\,\nu} \tag{3.5}$$

The *true anomaly* ν, the *semi-major axis* a and the *eccentricity* e are defined in figure 3.6 and in figures 2.2–2.4 of chapter 2. The eccentricity e can be expressed as a function of the semi-major axis a and of the radii of apocentre and pericentre, r_{a} and r_{p}:

$$\begin{array}{rcl} r_{\mathrm{p}} & = & a(1-e) \\ r_{\mathrm{a}} & = & a(1+e) \end{array} \tag{3.6}$$

In an Earth orbit, apocentre and pericentre are called apogee and perigee.

The rate of the true anomaly can be derived from Kepler's second law, $h = \sqrt{\mu\,p} = \sqrt{\mu a(1-e^2)}$, and the specific angular momentum of the orbit, $h = \dot{\nu} r^2$. With these relations and r from Eq. (3.5), one obtains

$$\dot{\nu} = (1+e\,\cos\,\nu)^2 \sqrt{\frac{\mu}{a^3(1-e^2)^3}} \tag{3.7}$$

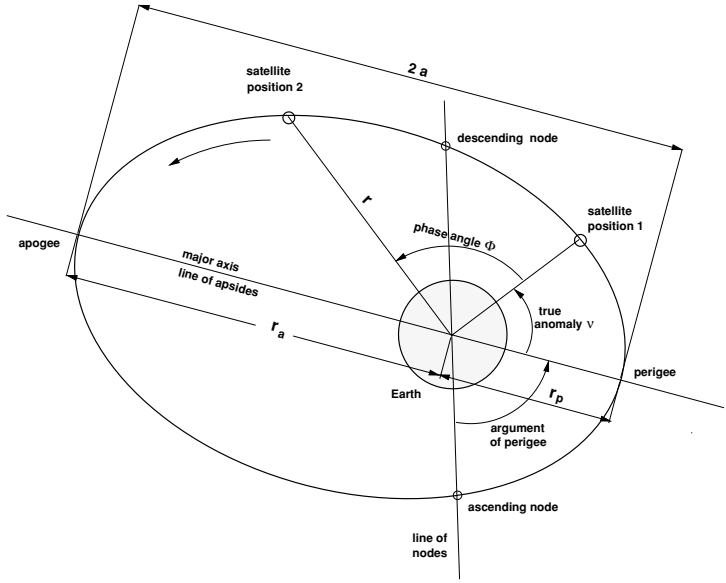

Figure 3.6. Definition of orbital elements in an Earth orbit.

The orbital period of an elliptic orbit can be derived from Eq. (3.7) by integration over one orbital revolution:

$$T = 2\pi\sqrt{\frac{a^3}{\mu}} \tag{3.8}$$

From Eq. (3.8) a mean motion n of an elliptical orbit can be defined as

$$n = \frac{2\pi}{T} = \sqrt{\frac{\mu}{a^3}} \tag{3.9}$$

From the energy conservation law, $E = \frac{V^2}{2} - \frac{\mu}{r} = -\frac{\mu}{2a}$, the velocity in the orbit direction can be derived:

$$V = \sqrt{\mu\left(\frac{2}{r} - \frac{1}{a}\right)} \tag{3.10}$$

The change of the mean phase difference between chaser and the target over time is $\Delta\Phi = (n_\mathrm{c} - n_\mathrm{t})\Delta t$. Per orbital revolution of the target, the phase advance of the chaser becomes, with Eq. (3.9),

$$\Delta\Phi = 2\pi\left(\frac{1}{T_\mathrm{c}} - \frac{1}{T_\mathrm{t}}\right)T_t = 2\pi\left(\frac{T_\mathrm{t}}{T_\mathrm{c}} - 1\right) \tag{3.11}$$

where T_t is the orbital period of the target and T_c is the period of the chaser.

Circular orbits

Most important for the application to rendezvous trajectories is the special case of the circular orbit, as practically all of the rendezvous missions are performed in near circular low Earth orbits (LEO). By setting $a = r$ and $e = 0$, the equations for the circular orbit can be obtained from the above equations for elliptic orbits as follows.

The rate of the true anomaly in a circular orbit is equal to the angular velocity of the orbit $\omega = \dot{\nu}$:

$$\omega_{\odot} = \sqrt{\frac{\mu}{r^3}} \tag{3.12}$$

The velocity in a circular orbit is

$$V_{\odot} = \sqrt{\frac{\mu}{r}} \tag{3.13}$$

and the orbital period is

$$T_{\odot} = 2\pi\sqrt{\frac{r^3}{\mu}} \tag{3.14}$$

3.2.2 Orbit corrections

The discussion of orbit corrections in this section assumes that all manoeuvres are impulsive, i.e. that they consist of an instantaneous change of velocity at the point where the manoeuvre is applied. This is a first approximation, which is convenient and sufficient to explain the effects in principle. Accurate manoeuvre calculation needs to take into account the maximum thrust level available and the necessary duration of the thrust to achieve the required ΔV.

Apogee and perigee raise manoeuvres

A tangential thrust at perigee in the direction of the orbital velocity vector will increase the semi-major axis of the orbit and thus raise the apogee. With Eq. (3.10) the ΔV required to achieve the new semi-major axis a_2 becomes

$$\Delta V_{\mathrm{p}} = V_{\mathrm{p}2} - V_{\mathrm{p}1} = \sqrt{\mu}\left(\sqrt{\frac{2}{r_{\mathrm{p}}} - \frac{1}{a_2}} - \sqrt{\frac{2}{r_{\mathrm{p}}} - \frac{1}{a_1}}\right) \tag{3.15}$$

$V_{\mathrm{p}1}$ and $V_{\mathrm{p}2}$ are the velocities at perigee before and after the manoeuvre. To raise the perigee, a corresponding tangential thrust in apogee in the direction of the orbital velocity vector must be provided:

$$\Delta V_{\mathrm{a}} = V_{\mathrm{a}2} - V_{\mathrm{a}1} = \sqrt{\mu}\left(\sqrt{\frac{2}{r_{\mathrm{a}}} - \frac{1}{a_2}} - \sqrt{\frac{2}{r_{\mathrm{a}}} - \frac{1}{a_1}}\right) \tag{3.16}$$

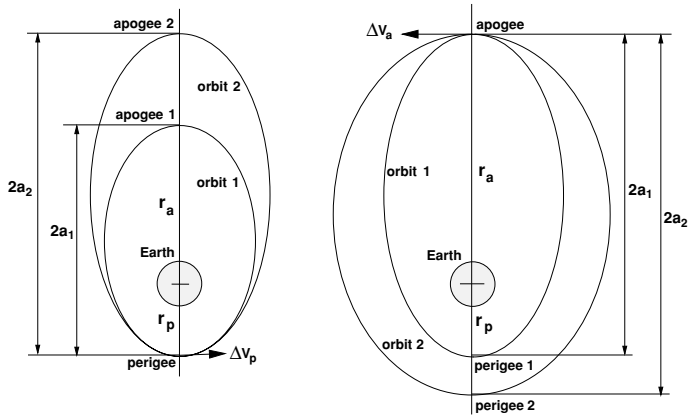

Figure 3.7. Apogee and perigee raise manoeuvres.

$V_{\mathrm{a}1}$ and $V_{\mathrm{a}2}$ are now the velocities at apogee before and after the manoeuvre. Remembering that $r_{\mathrm{p}} = a(1-e)$ and $r_{\mathrm{a}} = a(1+e)$, it can be seen that an increase of velocity at perigee will increase the eccentricity of the orbit, and an increase of velocity at apogee will decrease it.

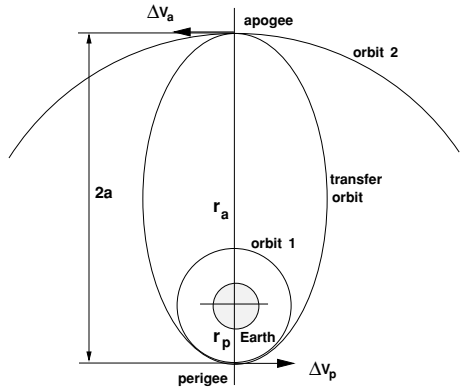

Figure 3.8. Orbit relations in a Hohmann transfer.

When starting and ending at circular orbits the combined perigee and apogee manoeuvres become the well known *Hohmann transfer* (Hohmann 1925) (figure 3.8). With Eqs. (3.10) and (3.13) one obtains

$$\Delta V_{\mathrm{p}} = \sqrt{\mu\left(\frac{2}{r_1} - \frac{1}{a}\right)} - \sqrt{\frac{\mu}{r_1}} \tag{3.17}$$

and

$$\Delta V_{\mathrm{a}} = \sqrt{\frac{\mu}{r_2}} - \sqrt{\mu\left(\frac{2}{r_2} - \frac{1}{a}\right)} \tag{3.18}$$

The semi-major axis of the transfer ellipse is

$$a = \frac{r_1 + r_2}{2} \tag{3.19}$$

Correction of inclination and RAAN errors

The plane of an orbit is given by the inclination i and the right ascension of ascending node (RAAN) Ω, as defined in figure 2.2. For a pure change of the orbital plane, the ΔV must be applied perpendicular to the plane. Any component in the orbit plane will lead to a change of eccentricity or orbit size or both. Further, since the new orbit will go through the point at which the manoeuvre has been applied, the correction ΔV must be applied at the intersection of the initial orbit with the intended one. So, for a change of inclination, the ΔV must be applied at the ascending or descending node, and for a change of RAAN it must be applied at half the arc between those nodes.

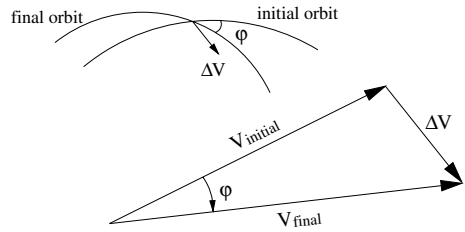

Figure 3.9. Corrections of orbital plane.

However, since pure plane change manoeuvres are relatively expensive, plane angle corrections are usually combined with in-plane transfer manoeuvres. With the cosine law one obtains

$$\Delta V = \sqrt{V_{\mathrm{i}}^2 + V_{\mathrm{f}}^2 - 2V_{\mathrm{i}}V_{\mathrm{f}}\cos\varphi} \tag{3.20}$$

where φ is the angle between the initial and the final orbit plane (see figure 3.9). The need for plane corrections arises mainly from the launch errors and from the drift of nodes due to the J_2-disturbance (see section 4.2.3).

A detailed discussion of the launch and phasing orbit manoeuvres has been provided by J. Legenne in Carrou (1995).

3.2.3 The equations of motion in the target reference frame

The equations of orbital motion discussed in section 3.2.1 are given in the orbital plane frame $\boldsymbol{F}_{\mathbf{op}}$. Equations of motion in this frame can conveniently be used for trajectory analysis until the chaser vehicle is in the close vicinity of the target. For relative navigation it becomes more convenient to keep one of the spacecraft as a fixed point. For the analysis of rendezvous trajectories, it is best to use a reference frame originating in the CoM of the target vehicle, i.e. to look at the chaser motion as an astronaut sitting in the target vehicle would. This frame is the spacecraft local orbital frame of the target, $\boldsymbol{F}_{\mathbf{lo}}$, defined in section 3.1.

For circular orbits the equations of relative motion are the Hill equations (see also appendix A):

$$\begin{aligned} \ddot{x} - 2\omega\dot{z} &= \frac{1}{m_\mathrm{c}} F_x \\ \ddot{y} + \omega^2 y &= \frac{1}{m_\mathrm{c}} F_y \\ \ddot{z} + 2\omega\dot{x} - 3\omega^2 z &= \frac{1}{m_\mathrm{c}} F_z \end{aligned} \tag{3.21}$$

In these equations $\omega = \frac{2\pi}{T}$ is the angular frequency of the circular target orbit and m_c is the mass of the chaser vehicle. The motion can be disturbed by imposed accelerations $\gamma_{x,y,z} = \frac{F_{x,y,z}}{m_\mathrm{c}}$. Eqs. (3.21) are a system of linear differential equations, which can be solved using the Laplace transformation method. For distances between chaser and target vehicles that are very small compared with the distance to the centre of the Earth, a linearised solution of the equations of relative motion has been derived from the Hill equations by W. H. Clohessy and R. S. Wiltshire (Clohessy & Wiltshire 1960).

A derivation of the Clohessy–Wiltshire equations from Eqs. (3.21) can be found in appendix A both for the homogeneous solution (no input forces) and for a particular solution, where the special case of input pulses with constant amplitudes is considered. This case is of particular interest for spacecraft applications, as practically all gas jet thrusters produce pulses of constant amplitude. Unfortunately this particular solution leads to relatively long mathematical expressions, which can be well processed by computers, but are less perceptual in the discussion of trajectory properties. For ease of discussion of the various trajectory types, it has been assumed that thrust manoeuvres are of an impulsive nature, i.e. step changes of velocity, and that longer term accelerations $\gamma_{x,y,z}$, whether resulting from thruster activities or from external disturbances, are constant over the time period considered. The constant force solution can be seen as a special case of Eqs. (A.43)–(A.47) and can be obtained by setting the start time of the pulse $t_1 = 0$ and the stop time $t_2 = t$. The resulting equations of motion for constant

input forces are

$$\begin{aligned} x(t) &= \left(\frac{4\dot{x}_0}{\omega} - 6z_0\right)\sin(\omega t) - \frac{2\dot{z}_0}{\omega}\cos(\omega t) + (6\omega z_0 - 3\dot{x}_0)t + \left(x_0 + \frac{2\dot{z}_0}{\omega}\right) + \cdots \\ &\quad + \frac{2}{\omega^2}\gamma_z(\omega t - \sin(\omega t)) + \gamma_x\left(\frac{4}{\omega^2}(1-\cos(\omega t)) - \frac{3}{2}t^2\right) \\ y(t) &= y_0\cos(\omega t) + \frac{\dot{y}_0}{\omega}\sin(\omega t) + \frac{\gamma_y}{\omega^2}(1-\cos(\omega t)) \\ z(t) &= \left(\frac{2\dot{x}_0}{\omega} - 3z_0\right)\cos(\omega t) + \frac{\dot{z}_0}{\omega}\sin(\omega t) + \left(4z_0 - \frac{2\dot{x}_0}{\omega}\right) + \cdots \\ &\quad + \frac{2}{\omega^2}\gamma_x(\sin(\omega t) - \omega t) + \frac{\gamma_z}{\omega^2}(1-\cos(\omega t)) \end{aligned} \tag{3.22}$$

Because of the linearisation, the accuracy of the Clohessy–Wiltshire (CW) equations decreases with the distance from the origin of the coordinate-ordinate frame. In a LEO rendezvous mission, position errors will become significant at a distance of a few tens of kilometres from the origin. For example, the error in the z-direction due to the curvature of the orbit will be $\Delta z = r(1 - \cos\frac{x}{r})$, which for an orbit with $h = 400$ km, $r = 6766$ km at a distance of $x = 10$ km, becomes $\Delta z = 7.4$ m, and at a distance of $x = 30$ km becomes $\Delta z = 66.5$ m. If a curved definition of the x-coordinate were used, according to the actual circular orbit, the useful range of the CW equations can be significantly increased.

Many attempts have been made to solve the Hill equations (3.21) also for elliptical orbits (Wolfsberger 1983; Carter 1998). An elegant solution has been described in Yamanaka & Ankersen (2002), which includes the CW equations as a special case for zero eccentricity. The treatment of elliptical orbits is, however, outside the scope of this book, as practically all rendezvous missions are in circular orbit and as discussing the elliptical cases would not add anything to the basic understanding of trajectories of current rendezvous missions.

3.3 Discussion of trajectory types

The objective of this section is to describe the motion of the chaser spacecraft, and other properties of the chaser trajectory, in order to provide the basis for the discussion of trajectory safety and of approach/departure strategies in later chapters. For all trajectory discussions hereafter, the $\boldsymbol{F}_{\mathrm{lo}}$ frame of the target will be used. The trajectory elements can be grouped for the purpose of this discussion into three types:

- *Free drift trajectories*: these are trajectories evolving from a set of initial conditions for position and velocity, without application of thrust impulses or forces.
- *Impulsive manoeuvre trajectories*: these are trajectories evolving from a set of initial conditions plus an instant change of velocity, representing a boost manoeuvre.

- *Continuous thrust trajectories*: these are trajectories evolving from a set of initial conditions plus the continuous application of control forces (open loop) along the trajectory.

This grouping is somewhat arbitrary, as for the trajectory dynamics, e.g., it does not make any difference whether a certain velocity was present as an initial condition at the starting time t_0, or whether it has been applied as a step function at the time t_0. Also, boost manoeuvres are in reality not purely impulsive manoeuvres. In fact, with a limited thrust level available, thrust forces have to be applied over a certain time to achieve a certain ΔV. The grouping applied here is motivated rather by the typical questions in practical applications, where one would like to know: (a) the trajectory evolution when no impulses or forces are applied, (b) the trajectory evolution when a particular thrust manoeuvre is applied, or (c) the impulses or forces which need to be applied when certain trajectories shall be achieved.

The trajectory types discussed are intended to cover the most important types used in rendezvous approach and departure missions. However, whereas in a real mission a large part of the trajectories may be closed loop controlled and/or will be subject to external and internal disturbances, the trajectories in this section are treated as ideal open loop cases, without any disturbances. Trajectory deviations as a result of external and internal disturbances are discussed in sections 4.2 and 4.3.

For each trajectory type discussed in the following sections of this chapter,

- the assumed initial conditions,
- the equations of motion,
- the position after a fixed time (e.g. half or one orbital revolution),
- or, where applicable, the duration of a transfer to a certain position

will be derived. For free drift and impulsive manoeuvre cases, one example of a plot of each type of trajectory will be given and its characteristics discussed. Further, for impulsive and continuous force manoeuvres the required ΔV will be derived. Application examples will be given for all trajectories addressed.

Note: In general trajectory drawings the $+x$-direction (+V-bar) points to the left and the $+z$-direction (+R-bar) points downwards. This is in accordance with the convention used in the ISS scenario. For the example plots, which are produced using the $MATRIX_x$ tool, the x-direction (+V-bar) is pointing in the usual way to the right, but the z-direction (+R-bar) points upwards. The examples shown in the plots are calculated for 400 km altitude circular orbits.

3.3.1 Free drift motions

In this section, four cases will be discussed, selected because of their significance as elements of approach and departure strategies in rendezvous missions. These are

- the motion on a coplanar orbit at different altitude;
- the release from a station at a positive or negative distance in the z-direction (R-bar) from the CoM of the station;
- the release from a station at a positive or negative distance in the y-direction (H-bar) from the CoM of the station;
- the release (inhibit of control) from a forced motion along the target orbit or along the radius vector.

In all four cases no thrust manoeuvre is applied to the orbit at the initial point of the trajectory section under discussion. Except for the first one, in all cases there is, however, an instantaneous change of conditions assumed to take place at the initial trajectory point.

Relative motion on orbit with different altitude

This is the case of a chaser moving coplanar with the target in an orbit slightly lower or higher than the target orbit. The difference between the angular frequency of a chaser orbit w.r.t. the target orbit can be obtained for small differences by differentiation of Eq. (3.12):

$$\omega = \sqrt{\frac{\mu}{r^3}}$$

$$\mathrm{d}\omega = -\frac{3}{2r}\omega \mathrm{d}r \tag{3.23}$$

In the $\boldsymbol{F}_{\mathbf{lo}}$ frame of the target $\mathrm{d}z = -\mathrm{d}r$.

Further, by defining $\omega_\mathrm{t} = \omega$ of target and $\omega_\mathrm{c} = \omega$ of chaser, and replacing $\mathrm{d}\omega$ in Eq. (3.23) by $\Delta\omega = (\omega_\mathrm{t} - \omega_\mathrm{c})$, and setting $\Delta\omega r = \dot{x}$ and $\mathrm{d}z = z_\mathrm{c}$, the velocity of a chaser becomes

$$\dot{x}_\mathrm{c} = \frac{3}{2}\omega_\mathrm{t} z_\mathrm{c} \tag{3.24}$$

With this relation for a free orbit motion at a different altitude, the following initial conditions can be defined:

$$\begin{array}{rclrcl} x_0, y_0 & = & 0 & \dot{x}_0 & = & \frac{3}{2}\omega Z_0 \\ z_0 & = & Z_0 & \dot{y}_0, \dot{z}_0 & = & 0 \end{array}$$

Inserting the initial conditions into Eqs. (3.22), the equations of motion become for this case:

$$\begin{array}{rcl} x(t) & = & \frac{3}{2}\omega Z_0 t \\ y(t) & = & 0 \\ z(t) & = & Z_0 \end{array} \tag{3.25}$$

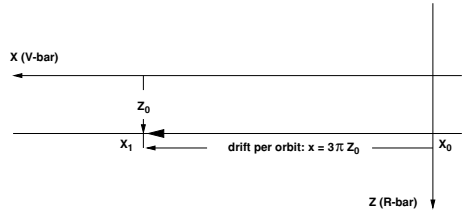

Figure 3.10. Coplanar motion at different orbital height.

After one orbital period of the target ($t = T$, $\omega t = 2\pi$) the advance of the chaser w.r.t. the target in the orbit direction is, as shown in figure 3.10:

$$X_T = 3\pi Z_0$$

This is a motion parallel to the target orbit with the relative velocity of $V_x = \frac{3}{2}\omega Z_0$. In rendezvous approach strategies, this type of trajectory can be used where a motion toward the target in the orbit direction together with a safe distance in the z-direction is required for safety reasons.

The motion due to different orbital height is de-coupled from the eccentricity and out-of-plane motions, i.e. the above result can be added to the equations of motion of all cases for $z_0 = 0$ to obtain the solution for initial conditions with a difference in altitude $z_0 = Z_0$.

Release at a distance from the station CoM in the z-direction

This is the case of a vehicle starting above or below the target orbit with the velocity of the target. Such a case can be imagined by considering a vehicle which was attached to the target structure at a distance Z_0 from the CoM and was subsequently released at time $t = t_0$. The initial conditions are then:

$$\begin{aligned} x_0, y_0 &= 0 \\ z_0 &= Z_0 \end{aligned} \qquad \dot{x}_0, \dot{y}_0, \dot{z}_0 = 0$$

Inserting the initial conditions into Eqs. (3.22), the equations of motion become for this case:

$$\begin{aligned} x(t) &= 6Z_0(\omega t - \sin(\omega t)) \\ y(t) &= 0 \\ z(t) &= Z_0(4 - 3\cos(\omega t)) \end{aligned} \tag{3.26}$$

After one orbital period of the target, the advance in orbit direction is

$$\begin{aligned} x_T &= 12\pi Z_0 \\ z_T &= Z_0 \end{aligned}$$

The cyclic motion with the orbital period T has an amplitude of $6Z_0$, i.e. starting at Z_0, arriving after $T/2$ at $7Z_0$ and returning after T to Z_0. The average z-distance of this orbit is

$$z_{\mathrm{m}} = 4z_0$$

which, inserted into Eqs. (3.25), yields the same result after one revolution, $x_T = 12\pi Z_0$, as above.

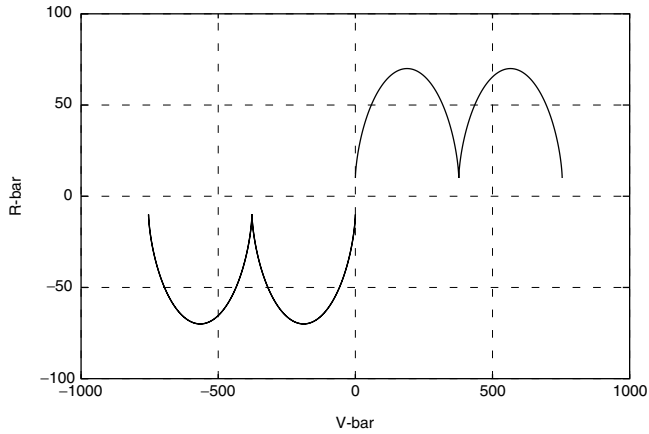

Figure 3.11. Example: trajectories after release at $Z_0 = +10$ m and $Z_0 = -10$ m.

The example shown in figure 3.11 indicates the significant effects caused by orbit dynamics for a release at small z-distances from the target orbit. Two examples are shown with a release distance of $Z_0 = +10$ m (below target CoM) and $Z_0 = -10$ m (above target CoM). After half an orbit the trajectory has reached a z-distance of 70 m, and after one orbit it has reached an x-distance of 377 m, where the trajectory starting above the target orbit $(-z)$ moves backward, and the one starting at a $+z$-position moves forward w.r.t. the target.

This result is very interesting for departure operations because of the significant advance in the x-direction. An application example for this trajectory case is the undocking of a vehicle from a port above or below the target orbit, or the release by a manipulator arm, at a distance in the $\pm z$-direction from the CoM of the station.

Release at a distance from the station CoM in the *y*-direction

This is the case of a vehicle moving at an out-of-plane distance to the target orbit with the velocity of the target. Again, such a case can be imagined by consideration of a vehicle which was attached to the target structure at a distance Y_0 from the CoM and

was released at time $t = t_0$. The initial conditions for the simplest case are:

$$\begin{aligned} x_0, z_0 &= 0 \\ y_0 &= Y_0 \end{aligned} \qquad \dot{x}_0, \dot{y}_0, \dot{z}_0 = 0$$

Inserting the initial conditions into Eqs. (3.22), the equations of motion are

$$\begin{aligned} x(t) &= 0 \\ y(t) &= Y_0 \cos(\omega t) \\ z(t) &= 0 \end{aligned} \tag{3.27}$$

The result is the expected pure sinusoidal motion starting with Y_0. As this motion is de-coupled from the in-plane motions, this result can be superimposed to all in-plane cases.

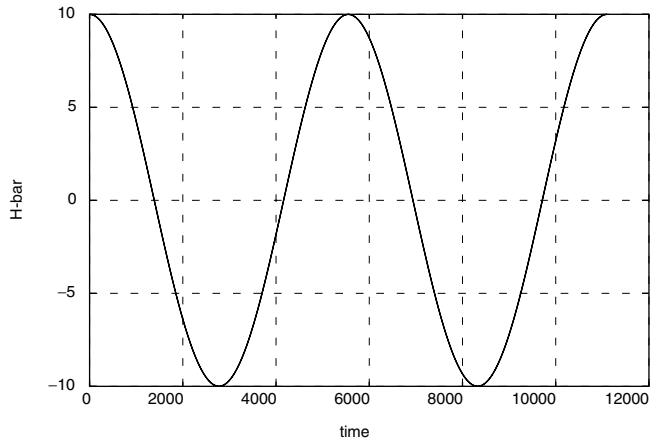

Figure 3.12. Example: motion over time after release at an out-of-plane distance of $Y_0 = 10$ m.

The example in figure 3.12 depicts the motion of a body after the release at a y-distance of $Y_0 = 10$ m from the target orbit (target CoM). If there are no obstacles, the body will pass the target orbit after a quarter orbit with a velocity of $\dot{y} = -Y_0 \cdot \omega = -0.0138$ m/s. After half an orbit it will reach the opposite extreme position of $y = -10$ m and after one orbit it will return to the initial position.

Again, this could be the case of a release by a manipulator arm of a departing vehicle at an out-of-plane distance Y_0 from the CoM of a space station. As a body to be released under these conditions tends to move along the y-axis toward the CoM of the vehicle, from where it is released, the above initial conditions would of course be meaningful only if the manipulator can easily establish the necessary distances X_0 or Z_0 to break free from the structure of the station.

Release from a forced motion along the target orbit (V-bar) or along the radius vector (R-bar)

These 'releases' are, e.g., the cases of thrust inhibit during forced motion straight line approaches on V-bar or R-bar (treated in section 3.3.3). When the continuous thrust necessary to implement the straight line trajectory is stopped at a certain point, the vehicle continues to move on V-bar, or on R-bar, respectively, with a velocity that is different from that belonging to a circular orbit of this altitude. As a result the Coriolis forces will move the vehicle away from the approach line, i.e. from the x-axis in the case of a V-bar approach, and from the z-axis in the case of an R-bar approach. Examples of such release trajectories are shown in figure 3.13 for V-bar and in figure 3.14 for R-bar.

Since there is no difference for the evolution of the trajectory whether a velocity is applied as a ΔV at the starting time t_0, or is present as an initial condition, the equations of motion are the same as those for impulsive manoeuvres, i.e. Eqs. (3.28) for the V-bar approach case and Eqs. (3.34) for the R-bar approach case given in section 3.3.2. In the case of a release at an initial z-position different from $Z_0 = 0$, the motion due to a different altitude, see Eqs. (3.25), has to be added.

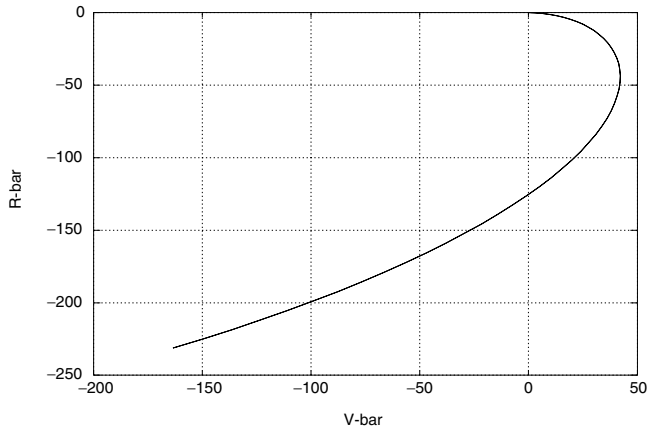

Figure 3.13. Example: release on V-bar with $V_x = +0.1$ m/s.

The example in figure 3.13 shows the free drift after thrust inhibit during a straight line approach along V-bar with a velocity of $\dot{x} = +0.1$ m/s. The resulting drift trajectory continues first to move forward, but at the same time it starts to move upward ($-z$-direction $= -$R-bar) and eventually backward ($-x$-direction $= -$V-bar). With the assumed initial velocity, it will touch again the target orbit after one orbital revolution at a distance of $x_T = -1656$ m. The maximum travel in the positive x-direction would be of the order of 45 m. The trajectory type is identical to the one shown in figures 3.15 and 3.17. The use of this type of trajectory to achieve passive trajectory safety w.r.t. collision is discussed in section 4.4.2 and is shown in figure 4.14.

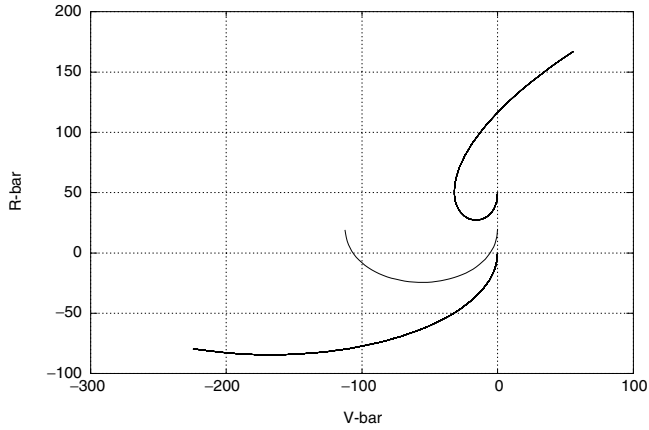

Figure 3.14. Example: release on R-bar with $V_z = -0.1$ m/s at $Z_0 = 0$, 20 m and 50 m.

Figure 3.14 shows three examples of drift trajectories after thrust inhibit during a straight line R-bar approach with a velocity of $\dot{z} = -0.1$ m/s. The difference between the three trajectories is the z-position at which thrust control is inhibited. For a release at $Z_0 = 0$ the trajectory is identical to the type described in figures 3.20 and 3.21. For the releases at $Z_0 = 20$ m and $Z_0 = 50$ m, the trajectory is a combination of the types shown in figure 3.11 (release at a z-distance) and figure 3.20 (impulse in z-direction), i.e. an addition of Eqs. (3.26) and (3.34). Whereas the trajectory in the case of a release at $Z_0 = 0$ will return after one orbital revolution to its starting point, in the other two cases with $Z_0 \neq 0$ a looping motion is initiated, which will result after one revolution in an x-distance from the release point. This behaviour can again be exploited for passive trajectory protection against collision (see section 4.4.2).

3.3.2 Impulsive manoeuvres

Thrust manoeuvres, to a first approximation, can be treated as impulses, i.e. as instantaneous changes of velocity at the time of manoeuvre. The acceleration terms of the CW equations can, therefore, be set to zero. In reality, due to limitations of thrust level available, such ideal impulsive manoeuvres do not exist and constant thrust forces have to be applied over a particular time to realise the manoeuvre (see section 3.3.3). The ideal case of a pure impulse allows us, however, to calculate manoeuvres easily, analyse manoeuvre strategies and assess the minimum ΔV required. As mentioned above, with the assumption of pure impulses, the equations of motion for impulsive manoeuvres are identical to the ones for the cases of 'release to free drift', where the initial velocity is different from that belonging to a circular orbit at the point of release.

Within this section the cases of impulsive manoeuvres with ΔV values in orbital and in radial directions will be discussed. Examples will be shown of how a combination of

such manoeuvres can be applied in advance in an orbital direction to change the orbital height and to fly around a particular point in orbit, e.g. a target station. For each of the applications, the required ΔV and duration will be indicated and the particular advantages or disadvantages discussed.

ΔV in an orbital direction

Thrust manoeuvres with a ΔV in a $\pm\, x$-direction (tangential manoeuvres) are used for transfers along the target orbit, for transfers to an orbit of a different height and for fly-arounds, e.g. from V-bar to a point where an R-bar approach can commence.

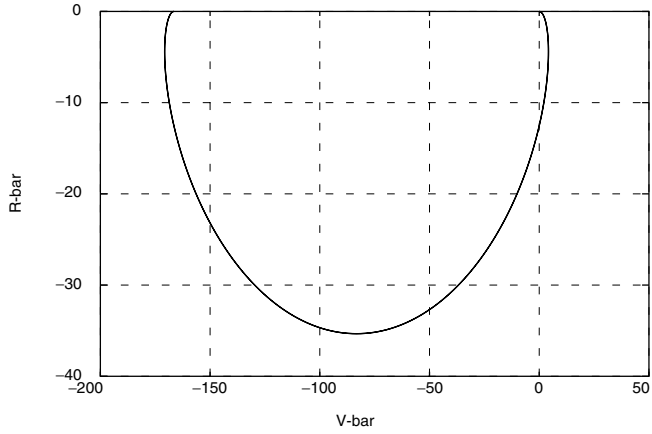

Figure 3.15. Example: impulse of $\Delta V_x = 0.01$ m/s, starting at $x = 0$, $z = 0$.

The simplest case is presented here, i.e. the manoeuvre takes place on the target orbit at the position of the target station $\boldsymbol{O_{lo}}$. The initial conditions are then:

$$x_0, y_0, z_0 = 0 \qquad \begin{aligned} \dot{x}_0 &= \Delta V_x \\ \dot{y}_0, \dot{z}_0 &= 0 \end{aligned}$$

Inserting the initial conditions into Eqs. (3.22), the equations of motion after a ΔV_x manoeuvre become:

$$\begin{aligned} x(t) &= \frac{1}{\omega}\Delta V_x(4\sin(\omega t) - 3\omega t) \\ y(t) &= 0 \\ z(t) &= \frac{2}{\omega}\Delta V_x(\cos(\omega t) - 1) \end{aligned} \tag{3.28}$$

Figure 3.15 shows an example of a trajectory after a tangential impulse in an orbit direction of $V_x = +0.01$ m/s, starting at $x = 0$, $z = 0$. The example indicates the

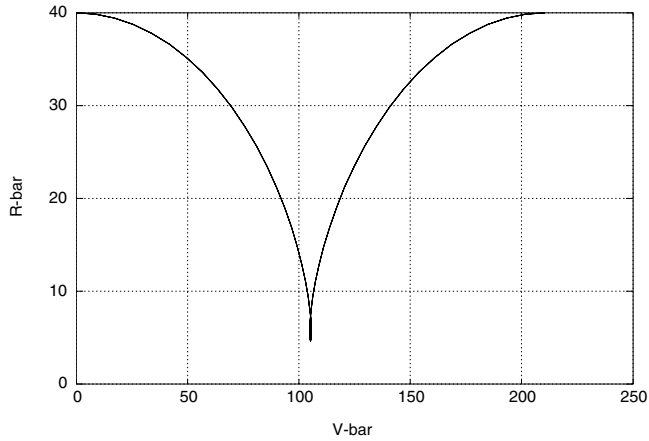

Figure 3.16. Example: impulse of $\Delta V_x = 0.01$ m/s, starting 40 m below target orbit.

sensitivity of the trajectory to velocity changes in orbit direction. A relatively small ΔV results in significant displacements, i.e. after half an orbital revolution more than 35 m in a $-z$-direction (above the initial orbit) and after one revolution more than 170 m in the $-x$-direction (behind the initial position).

ΔV_x on a higher or lower orbit than the target orbit The simple initial conditions which are used for Eqs. (3.28), i.e. all positions and all velocities (except for the applied ΔV) are zero, are of course not given in most cases of interest. For a position $x \neq 0$ the result is trivial, as in the CW equation for $x(t)$, Eqs. (3.22); the initial position x_0 is a constant, which will be added to each point of the motion, but has no further impact on the trajectory evolution. In contrast, for an initial position $z_0 \neq 0$, the additional relative velocity in the x-direction due to a different orbital altitude has to be taken into account. This motion is, however, independent from the other motions, as we have seen already in section 3.3.1. The initial conditions and equations of motion for the ΔV_x manoeuvre on a circular orbit of different altitude can therefore be obtained by adding to Eqs. (3.28) for the impulsive manoeuvre the equations for motion (3.25) at a different altitude. Figure 3.16 shows an example of how initial, non-zero, x- and z-positions influence the trajectory evolution.

The tangential impulse of $\Delta V_x = +1$ cm/s in the example of figure 3.16 is applied on an orbit that is $z = 40$ m below the target orbit. The result shows that the forward motion in the x-direction due to the z-distance of 40 m is predominant. In contrast to the example given in figure 3.15 for the same ΔV_x, the motion is now in the $+x$-direction, whereas the maximum displacement in the $-z$-direction is the same as in the previous case.

Applications of tangential thrust manoeuvres

Tangential impulse transfer along V-bar The principle of a transfer along V-bar by tangential thrusts is shown in figure 3.17. Starting at a point x_1 with a ΔV_{x1}, after one

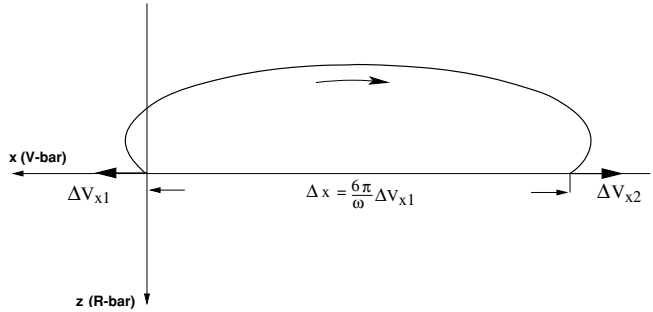

Figure 3.17. Transfer along V-bar by tangential impulses.

orbital period of the target, i.e. at $t = T$ and $\omega t = 2\pi$, the trajectory, Eqs. (3.28), has reached

$$\begin{aligned} x_T &= x_1 + \Delta x = x_1 - \frac{6\pi}{\omega}\Delta V_{x1} \\ z_T &= z_1 = 0 \end{aligned} \tag{3.29}$$

The required ΔV is accordingly

$$\Delta V_{x1} = -\frac{\omega}{6\pi}\Delta x \tag{3.30}$$

To come to a rest at the new position x_T on the target orbit, a stop impulse of the same size but in the opposite direction, $\Delta V_{x2} = -\Delta V_{x1}$, must be applied. The magnitude of the required ΔV in both cases is

$$|\Delta V_{x1}| = |\Delta V_{x2}| = \frac{\omega}{6\pi}\Delta x$$

The total ΔV expenditure for such a two-pulse manoeuvre is

$$\Delta V_{\text{total}} = \frac{\omega}{3\pi}\,\Delta x$$

Transfer to an orbit of different altitude To transfer a vehicle to an orbit of different altitude (see figure 3.18), the elliptical motion has to be stopped after half an orbital period, i.e. at $t = T/2$ and $\omega t = \pi$. Starting at x_1, z_1 with ΔV_{x1}, the trajectory,

Eqs. (3.28), has reached, after $t = T/2$, the maximum amplitude in z:

$$\begin{aligned} x_{T/2} &= x_1 + \Delta x = x_1 - \frac{3\pi}{\omega}\Delta V_{x1} \\ z_{T/2} &= z_1 + \Delta z = z_1 - \frac{4}{\omega}\Delta V_{x1} \end{aligned} \tag{3.31}$$

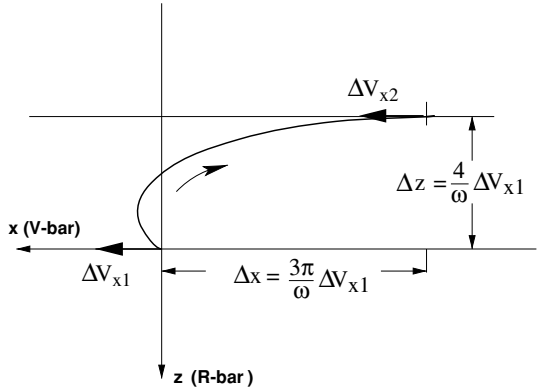

Figure 3.18. Transfer to orbit of different height (Hohmann transfer).

By the first impulse the new orbit becomes eccentric. To circularise it again at the altitude of $z_{T/2}$, an impulse of the same size and in the same direction must be applied (this is true only within the limitations of validity of the CW equations; for large differences in altitude, see Eqs. (3.17) and (3.18)). This manoeuvre is the well known *Hohmann transfer* already mentioned in section 3.2.2. Of interest for the design of trajectory strategies and operations is the fixed relation between the change of position in the z- and x-directions:

$$\Delta x = \frac{3\pi}{4}\Delta z$$

With $\Delta z = z_2 - z_1$, the magnitude of the required ΔV in both cases results from Eqs. (3.31):

$$\Delta V_{x1} = \Delta V_{x2} = \frac{\omega}{4}\Delta z \tag{3.32}$$

The total ΔV required for such a two-pulse manoeuvre is

$$\Delta V_{\text{total}} = \frac{\omega}{2}\,\Delta z$$

Tangential impulse fly-around manoeuvre For a fly-around to an R-bar approach (see figure 3.19), the same manoeuvres have to be applied as for the transfer to a different altitude. In order to arrive at the docking axis ($x = 0$) without a velocity in the z-

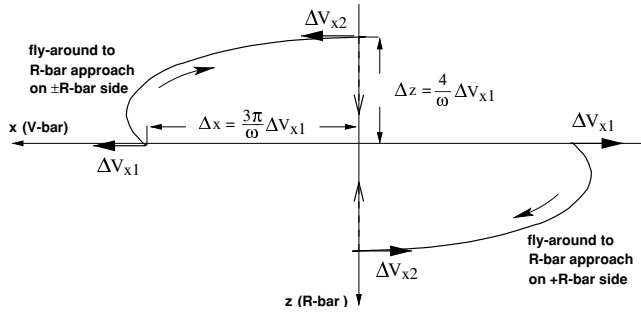

Figure 3.19. Fly-around by tangential impulse

direction ($V_z = 0$), the first pulse has to be given at a position $x_1 = \pm\frac{3\pi}{\omega}\Delta V_x$ on V-bar and the second one at $x_2 = 0$ (see figure 3.19). After a second impulse ΔV_{x2}, which would just achieve circularisation, as in a Hohmann transfer, the vehicle would move with a velocity V_x belonging to an orbit of that particular altitude. For a straight line R-bar approach the velocity V_x must, however, be the same as that of the target station all along the trajectory. The difference between the velocity at the end of the Hohmann transfer and the target orbit is, according to Eq. (3.24), $\dot{x} = \frac{3}{2}\omega\Delta Z$. This is the amount that has to be added to the second impulse. With Eq. (3.32) the ΔV for the second pulse of a fly-around manoeuvre becomes

$$\begin{aligned} \Delta V_{x2} &= \frac{\omega}{4}\Delta z + \frac{3\omega}{2}\Delta z \\ &= \frac{7\omega}{4}\Delta z \end{aligned} \tag{3.33}$$

Together with, or immediately after, the second fly-around impulse, the R-bar approach manoeuvre or a station keeping manoeuvre (see section 3.3.3) has to be initiated. Otherwise the vehicle will start the motion shown in figure 3.11.

ΔV in a radial direction

Thrust manoeuvres with a ΔV in $\pm z$-direction (radial manoeuvres) can be used, similar to the tangential manoeuvres, for transfer along the target orbit and for fly-around to an R-bar approach. A particular property of radial manoeuvres is that they affect only the eccentricity, not the orbital period, and thus cause no drift w.r.t. the target orbit. The differences in transfer distances and ΔV cost are given below in the discussion of equivalent cases.

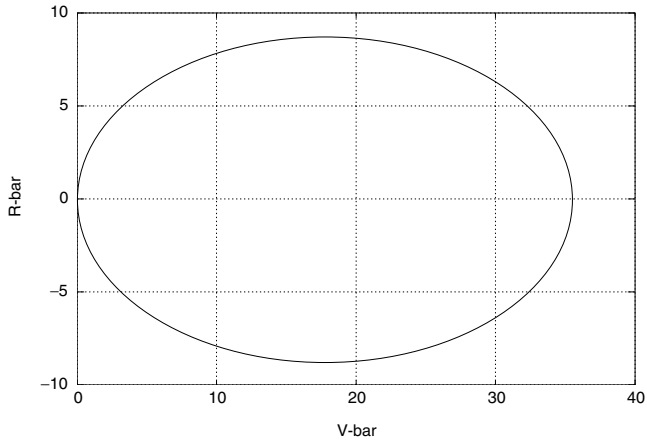

Figure 3.20. Example: impulse of $\Delta V_{z0} = 0.01$ m/s, starting on target orbit at $x = 0$.

For the simplest case of a manoeuvre starting in $\boldsymbol{O}_{\mathbf{lo}}$ the initial conditions are:

$$x_0, y_0, z_0 = 0 \qquad \begin{aligned} \dot{x}_0, \dot{y}_0 &= 0 \\ \dot{z}_0 &= \Delta V_z \end{aligned}$$

Inserting the initial conditions into Eqs. (3.22), the equations of motion become

$$\begin{aligned} x(t) &= \frac{2}{\omega}\Delta V_z(1 - \cos(\omega t)) \\ y(t) &= 0 \\ z(t) &= \frac{1}{\omega}\Delta V_z \sin(\omega t) \end{aligned} \tag{3.34}$$

In the $\boldsymbol{F}_{\mathbf{lo}}$ frame this trajectory is an ellipse, i.e. it returns to its starting point after each orbital revolution. After half an orbital period, i.e. at $t = T/2$ and $\omega t = \pi$, the trajectory, Eqs. (3.34), has reached its maximum amplitude in x:

$$\begin{aligned} x_{T/2} &= \frac{4}{\omega}\Delta V_z \\ z_{T/2} &= 0 \end{aligned} \tag{3.35}$$

The maximum amplitude in z has been reached after $t = T/4$:

$$z_{T/4} = \frac{1}{\omega}\Delta V_z \tag{3.36}$$

The example in figure 3.20 shows the behaviour described in Eqs. (3.34)–(3.36) for a small impulse in the z-direction of $\Delta V = +1$ cm/s, starting at an initial position of

$x = 0$, $z = 0$. In the first half of an orbital revolution, the trajectory moves in the $+z$-direction (below the initial orbit) and in the $+x$-direction; in the second half it moves in the opposite directions. The ratio of the maximum excursions in the x- and z-directions is $2:1$, as can be seen immediately from Eqs. (3.34). In comparison with figure 3.15 this example shows that the displacements due to a radial ΔV are much smaller than those due to a tangential ΔV of the same size, i.e. a factor of $\frac{2}{3\pi}$ (i.e. 35 m instead of 170 m) for the displacements in the x-direction and a factor of $\frac{1}{4}$ (i.e. 9 m instead of 35 m) for the ones in the z-direction.

Applications of radial thrust manoeuvres

Radial impulse transfer along V-bar Figure 3.21 shows the application of ΔVs in a radial direction as another possibility for a transfer to a different position on the target orbit. Starting at x_1, the transfer time to x_2 is half an orbital period $\left(\frac{T}{2}\right)$. To stop the motion at x_2, an impulse of the same size and direction, $\Delta V_{z1} = \Delta V_{z2}$, must be applied. With Eq. (3.35) and $\Delta x = x_2 - x_1$ the required ΔV in both cases becomes

$$\Delta V_{z1} = \Delta V_{z2} = \frac{\omega}{4}\Delta x \tag{3.37}$$

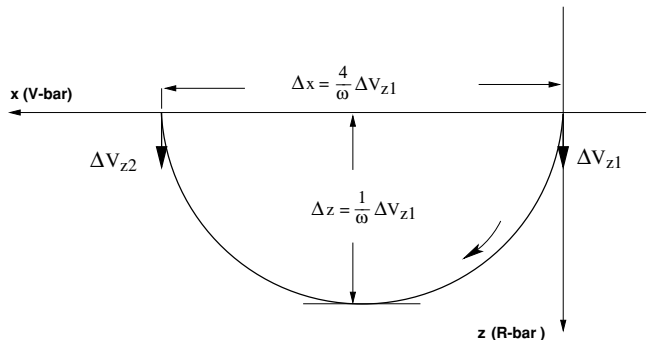

Figure 3.21. Transfer along V-bar by radial impulses.

The total ΔV required for such a two-pulse manoeuvre is

$$\Delta V_{\text{total}} = \frac{\omega}{2}\Delta x$$

In comparison with the transfer along V-bar by impulses in the orbit direction, the transfer by radial impulses is significantly more costly, i.e. by a factor of $\frac{3\pi}{2}$. Nevertheless, this transfer may be of interest because of safety and operational reasons (see chapters 4 and 5). One of the interesting features of this type of manoeuvre is the fact that, without the second impulse, the trajectory returns, if there are no disturbances, after one orbital revolution to its starting point. This allows, in the case of non-execution of the second boost, the repetition of the transfer trajectory without extra ΔV cost.

Radial impulse fly-around manoeuvre For a fly-around manoeuvre to an R-bar approach (see figure 3.22), the velocity component in the z-direction must be zero at arrival at the approach axis, i.e. the maximum amplitude $\Delta z = \frac{1}{\omega}\Delta V_{z1}$ of the trajectory (see Eq. (3.36)) must be reached at the beginning of an R-bar approach corridor at $x_2 = 0$. For a $\pm$ R-bar approach, the first pulse ΔV_{z1} must then be applied at a position $x_1 = \pm\frac{2}{\omega}\Delta V_z$ on V-bar and the motion, Eqs. (3.34), has to be stopped at $x_2 = 0, t = \frac{T}{4}, \omega t = \pi/2$. The impulse necessary to stop the motion in the $\pm x$-direction is

$$|\Delta V_x| = 2|\Delta V_{z1}| \tag{3.38}$$

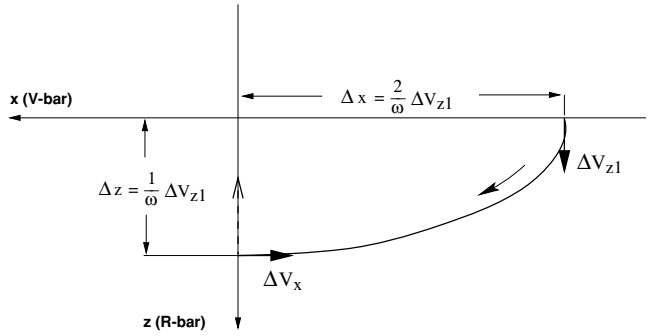

Figure 3.22. Fly-around by radial impulse.

The total ΔV required for such a fly-around manoeuvre is, with Eqs. (3.36) and (3.38),

$$\begin{aligned} \Delta V_{\text{total}} &= |\Delta V_{z1}| + |\Delta V_x| \\ \Delta V_{\text{total}} &= 3\Delta V_{z1} \end{aligned} \tag{3.39}$$

As in the case of the ΔV_x fly-around, together with, or immediately after, the second fly-around impulse of the ΔV_z fly-around, the R-bar approach manoeuvre or a station keeping manoeuvre (see section 3.3.3) has to be initiated. Otherwise the vehicle will start to describe the motion shown in figure 3.11.

ΔV in out-of-plane direction, orbit plane corrections

For the simplest case of a manoeuvre in $\boldsymbol{O}_{\mathbf{lo}}$ the initial conditions are

$$x_0, y_0, z_0 = 0 \qquad \begin{aligned} \dot{x}_0, \dot{z}_0 &= 0 \\ \dot{y}_0 &= \Delta V_y \end{aligned}$$

Inserting these initial conditions into Eqs. (3.22), the equations of motion become

$$\begin{aligned} x(t) &= 0 \\ y(t) &= \frac{1}{\omega}\Delta V_y \sin(\omega t) \\ z(t) &= 0 \end{aligned} \tag{3.40}$$

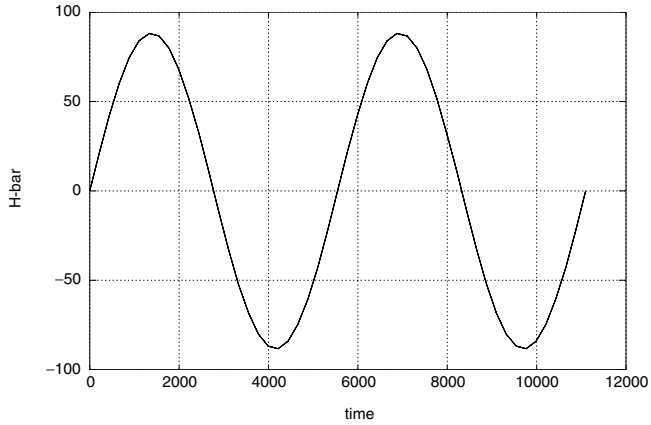

Figure 3.23. Impulse of $\Delta V_y = 0.1$ m/s, starting on target orbit.

The result is a pure sinusoidal motion starting with $y_0 = 0$. An example is shown in figure 3.23. The displacement in the y-direction is, for the same impulse, the same as the z-displacement for a radial impulse, shown in figure 3.20. The out-of-plane impulse does not cause displacements in other directions. As this motion is de-coupled from the in-plane motions, Eqs. (3.40) can be added to all in-plane cases.

Corrections of lateral motions can be performed, as has been shown in section 3.2.2, most efficiently at the intersection with the target orbit, i.e. when $y = 0$. In the rendezvous phase, when navigation is performed relative to the target in the $\boldsymbol{F}_{\mathbf{lo}}$ frame, there is no need to decompose the out-of-plane motion into inclination and RAAN components (which are used in the $\boldsymbol{F}_{\mathbf{eq}}$ frame to describe the orbit plane).

Impulsive transfer between arbitrary points (Lambert transfer)

In the previous sections, trajectory changes or transfers in one of the main directions of the local orbital frame have been discussed. Whereas out-of-plane manoeuvres are de-coupled from the two other axes, tangential and radial manoeuvres both produce trajectories with excursions in the x- and z-directions. The excursions have, however, different phasing over the orbital period, as we have seen in the previous sections. As a result, a combination of impulses in tangential and radial directions can be used if there

is a direct transfer between arbitrary points in the orbital plane. This type of transfer is known as a 'Lambert transfer'. The shape of the transfer trajectory depends not only on the x- and z-coordinates of the start and end points, but also on the time within which the transfer has to be performed. The required ΔVs in the x- and z-directions for the initial impulse to be applied at the position $x_0,\ z_0$ can be obtained by solving the CW equations (3.22) for $\dot{x}_0$ and $\dot{z}_0$:

$$\begin{aligned}\dot{x}_0 &= \frac{-\omega\sin(\omega t)(x-x_0)+\omega[6\omega t\sin(\omega t)-14(1-\cos(\omega t))]z_0+2\omega(1-\cos(\omega t))z}{3\omega t\sin(\omega t)-8(1-\cos(\omega t))}\\ \dot{z}_0 &= \frac{\omega[2(x_0-x)(1-\cos(\omega t))+(4sin(\omega t)-3\omega t\cos(\omega t))z_0+(3\omega t-4sin(\omega t))z]}{3\omega t\sin(\omega t)-8(1-\cos(\omega t))}\end{aligned} \tag{3.41}$$

by setting the chosen transfer time $t = t_1$, and by defining the initial velocities as

$$\begin{aligned}\dot{x}_0 &= V_{x0}+\Delta V_{x0}\\ \dot{z}_0 &= V_{z0}+\Delta V_{z0}\end{aligned}$$

V_{x0} and V_{z0} are the existing velocities prior to the application of the transfer impulses ΔV_{x0} and ΔV_{z0}.

The velocities at the final position $x_1,\ z_1$ can be obtained by differentiation of the CW equations (3.22), resulting in

$$\begin{aligned}\dot{x}(t_1) &= (4\dot{x}_0-6z_0\omega)\cos(\omega t_1)+2\dot{z}_0\sin(\omega t_1)+6z_0\omega-3\dot{x}_0\\ \dot{z}(t_1) &= (3z_0\omega-2\dot{x}_0)\sin(\omega t_1)+\dot{z}_0\cos(\omega t_1)\end{aligned} \tag{3.42}$$

and by inserting the chosen transfer time t_1 and the values found for $\dot{x}_0$ and $\dot{z}_0$ from Eqs. (3.41). The ΔVs for the second impulse at the position $x_1,\ z_1$ depend on the final velocity to be achieved. If the final condition is to be a point on a circular orbit, the final velocity in the local orbital frame of the target is given by Eq. (3.24). The ΔVs to be applied are

$$\begin{aligned}\Delta V_{x1} &= \frac{3}{2}\omega z_1-\dot{x}(t_1)\\ \Delta V_{z1} &= -\dot{z}(t_1)\end{aligned} \tag{3.43}$$

The evolution of the trajectory between the first and second ΔV can be calculated by inserting the assumed values for $x_0,\ z_0$ and the values calculated from Eqs. (3.41) for $\dot{x}_0,\ \dot{z}_0$ into the CW equations (3.22).

3.3.3 Continuous thrust manoeuvres

In this section a number of trajectories or manoeuvres will be addressed which, in contrast to all previous cases, need the application of continuous thrust forces in order to achieve a certain shape of trajectory or to keep a position. The following types of trajectories will be discussed:

- straight line trajectories on V-bar and R-bar;
- station keeping on different altitude and on out-of-plane distance w.r.t. the target;
- transfer by continuous thrust of limited level to a different altitude or to a different position along the target orbit;
- circular fly-around.

Whereas this is not an exhaustive list of trajectories with continuous thrust, the intention of this section is to address examples of the most important types of forced motion trajectories and to indicate how the equations for such cases can be derived.

Applications of straight line approach trajectories

Straight line trajectories are of interest for the final approach to the docking port or berthing position at the target station. With a straight line trajectory, lateral position errors in- and out-of-plane can easily be controlled w.r.t. the line of sight of a sensor. Also, monitoring of a straight line trajectory by human operators using direct eye sight or cameras will be easier than for a curved trajectory. Two general cases will be discussed for each approach direction: the special case of an approach with constant velocity and the general case of approaches with a pre-determined velocity profile. In real applications, straight line trajectories will always be closed loop controlled. The open loop solutions for simple trajectory and ΔV calculations are given below for the V-bar approach and in the subsequent section for the R-bar approach.

Straight line V-bar approach

Straight line V-bar approach with constant velocity This is the type of trajectory where a constant velocity of V_x w.r.t. the target is to be achieved between x_0 and x_1, with the velocities in the other directions kept zero. In the easiest case the motion is started with an impulse ΔV_{x1}, which produces the velocity in the x-direction V_x, and is stopped with an impulse of the same magnitude but in the opposite direction ΔV_{x2} (figure 3.24).

The initial conditions for the simplest case of a trajectory starting in x_0 are

$$\begin{array}{rrcll} x_0 = X_0 & \dot{x}_0 & = & \Delta V_{x1} & \\ y_0, z_0 = 0 & \dot{y}_0, \dot{z}_0 & = & 0 & \gamma_x, \gamma_y = 0 \end{array}$$

The equation of motion for $x(t) \in [x_0;\, x_1]$

$$x(t) = X_0 + V_x \cdot t \tag{3.44}$$

The force per mass unit γ_z that must be applied can be obtained from the Hill equations (3.21) by inserting the above assumed initial conditions:

$$\gamma_z = 2\omega V_x \tag{3.45}$$

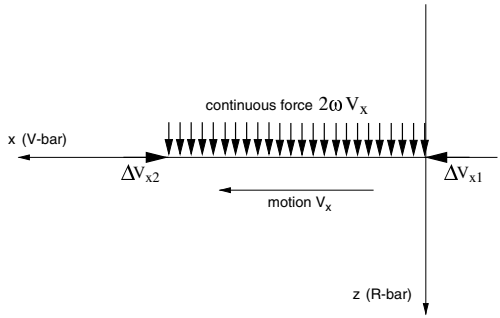

Figure 3.24. Straight line V-bar trajectory ($X_0 = 0$).

The total ΔV required for the transfer from x_0 to x_1 is

$$\Delta V_{\text{total}} = |\Delta V_x|_1 + |\gamma_z \Delta t| + |\Delta V_x|_2$$

The duration of the transfer is, with $\Delta x = x_1 - x_0$,

$$\Delta t = t_1 - t_0 = \frac{\Delta x}{V_x}$$

In reality, ΔV_{x1} and ΔV_{x2} will also be manoeuvres with a finite thrust and thrust duration, so that there will be a velocity profile (see the following section).

Straight line V-bar approach with velocity profile Assuming the initial conditions are the same as in the case above for constant velocity, the relations for a given velocity profile $V_x(t)$ are:

- The equation of motion for $x(t) \in [x_0;\, x_1]$

$$x(t) = x_0 + \int V_x(t)dt \tag{3.46}$$

- The force per unit of mass to be applied to keep the trajectory on the target orbit

$$\gamma_z(t) = 2\omega V_x(t) \tag{3.47}$$

- The total ΔV expenditure for the implementation of the velocity profile $V_x(t)$

$$\Delta V_{\text{total}} = \int_{t_0}^{t_1} \gamma_z(t)dt \tag{3.48}$$

Once the velocity profile $V(t)$ is defined, the equation of motion, the forces to be applied and the ΔV required can be calculated from the above equations.

Straight line R-bar approach

The special case of a constant velocity profile and the general case of a profile with changing velocity over time will be discussed.

Straight line R-bar approach with constant velocity At first, the velocity is assumed to be $V_z =$ constant between z_0 and z_1. Considering again the simplest case: the motion is started at z_0, t_0 with an impulse ΔV_{z1}, which produces the velocity in the z-direction V_{z1}, and is stopped at x_1, t_1 with an impulse ΔV_{z2} of the same magnitude but in the opposite direction (figure 3.25).

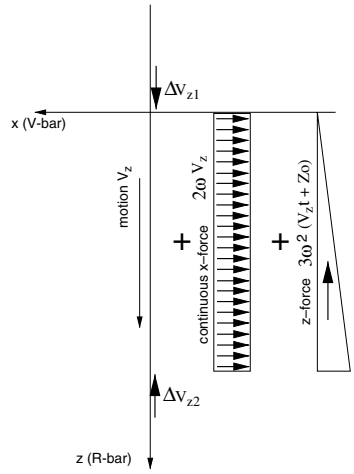

Figure 3.25. Straight line R-bar trajectory ($Z_0 = 0$).

The initial conditions for a trajectory starting in z_0 are

$$\begin{array}{rclrcl} x_0, y_0 & = & 0 & \dot{x_0}, \dot{y_0} & = & 0 \\ z_0 & = & Z_0 & \dot{z_0} & = & \Delta V_z \end{array} \qquad \gamma_y = 0$$

The equation of motion for $z(t) \in [z_0;\ z_1]$ is

$$z(t) = Z_0 + V_z \cdot t \tag{3.49}$$

The forces per unit of mass, γ_x and γ_z, which must be applied to counteract the orbital forces, can be obtained from the Hill equations (3.21) by inserting the above assumed initial conditions:

$$\begin{array}{rcll} \gamma_x & = & -2\omega V_z & (3.50) \\ \gamma_z & = & -3\omega^2(V_z t + Z_0) & \end{array}$$

The profiles for γ_x and γ_z are shown in figure 3.25. The total ΔV required for the transfer $z_0 - z_1$ is

$$\Delta V_{\text{total}} = |\Delta V_z|_1 + |\gamma_x \Delta t| + |\gamma_z \Delta t| + |\Delta V_z|_2$$

The duration of the transfer is, with $\Delta z = z_1 - z_0$,

$$\Delta t = t_1 - t_0 = \frac{\Delta z}{V_z}$$

Straight line R-bar approach with velocity profile Assuming the initial conditions are the same as in the case for constant velocity, the relations for a given velocity profile $V_z(t)$ are:

- the equation of motion for $z(t) \in [z_0; z_1]$

$$z(t) = z_0 + \int V_z(t) dt \tag{3.51}$$

- the forces per unit of mass to be applied to keep the trajectory on the target orbit

$$\begin{aligned} \gamma_x(t) &= -2\omega V_z(t) \\ \gamma_z(t) &= -3\omega^2 (V_z(t)t + Z_0) \end{aligned} \tag{3.52}$$

- the total ΔV expenditure for the implementation of the given velocity profile $V_z(t)$

$$\Delta V_{\text{total}} = |\int_{t_0}^{t_1} \gamma_x(t) dt| + |\int_{t_0}^{t_1} \gamma_z(t) dt| \tag{3.53}$$

As in the case for the straight line V-bar approach, once the velocity profile $V(t)$ is defined, the equation of motion, the forces to be applied and the ΔV required can be calculated from the above equations.

Station keeping on a position outside the target orbit

The attempted ideal conditions for station keeping are a fixed position w.r.t. the target and zero motion in any direction. For a position on the target orbit no control forces need to be applied. The cases to be discussed here are positions either at a different orbital height or at an out-of-plane distance. Station keeping elements of a trajectory sequence are usually closed loop controlled, as small errors in the assumed initial position and in the forces to be applied will lead to significant drift motions (see chapter 4). For this reason open loop station keeping manoeuvres can be applied only for short duration and at sufficient distance from the target station.

Station keeping below or above the target orbit The following initial conditions are assumed:

$$\begin{array}{rcll} x_0, y_0 & = & 0 & \dot{x_0}, \dot{y_0}, \dot{z_0} = 0 \qquad \gamma_x, \gamma_y = 0 \\ z_0 & = & Z_0 & \end{array}$$

The equations of motion are, by definition,

$$\begin{array}{r} x(t), y(t) = 0 \\ z(t) = Z_0 \end{array} \tag{3.54}$$

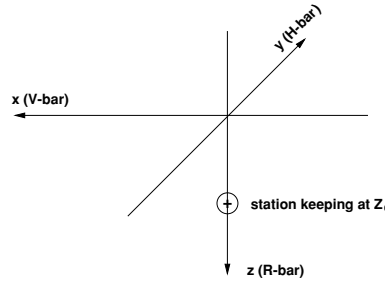

Figure 3.26. Station keeping below or above the target orbit.

The force per unit of mass γ_z, which must be applied to counteract the orbital forces, when a position below or above the target orbit is to be held, can be obtained from the Hill equations (3.21) by inserting the above initial conditions:

$$\gamma_z = -3\omega^2 Z_0 \tag{3.55}$$

The total ΔV required for station keeping at a position z_0 above or below the target orbit is

$$\Delta V_{\text{total}} = \gamma_z \Delta t = -3\omega^2 Z_0 \Delta t \tag{3.56}$$

The results are independent of the initial position x_0. The results for in-plane- and out-of-plane positions (see below) can be added for the case of a combined z_0, y_0 initial position.

Station keeping at out-of-plane position The following initial conditions are assumed:

$$\begin{array}{rcll} x_0, z_0 & = & 0 & \dot{x_0}, \dot{y_0}, \dot{z_0} = 0 \qquad \gamma_x, \gamma_z = 0 \\ y_0 & = & Y_0 & \end{array}$$

The equations of motion are accordingly

$$\begin{array}{rcl} x(t), z(t) & = & 0 \\ y(t) & = & Y_0 \end{array} \tag{3.57}$$

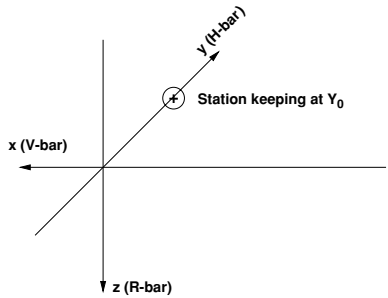

Figure 3.27. Station keeping at out-of-plane position.

The force per unit of mass γ_y, which must be applied to counteract the orbital forces, when an out-of-plane position is to be held, can be obtained for the above initial conditions from the Hill equations (3.21):

$$\gamma_y = \omega^2 Y_0 \tag{3.58}$$

The total ΔV required for station keeping at an out-of plane position Y_0 is

$$\Delta V_{\text{total}} = \gamma_y \Delta t = \omega^2 Y_0 \Delta t$$

Transfer by continuous *x*-thrust

In the impulsive manoeuvre cases discussed above (section 3.3.2), it has been assumed that the change of velocity is a step function. In reality all thrusters have a finite force level, so that a constant force has to be applied over a certain time in order to achieve a particular ΔV. A further case of interest concerning a constant force in the x-direction is the drag force of the residual atmosphere, which will be treated in more detail in section 4.2.1.

For the easiest case, with the trajectory starting in $\boldsymbol{O_{lo}}$, the initial conditions are

$$x_0, y_0, z_0 = 0 \qquad \dot{x_0}, \dot{y_0}, \dot{z_0} = 0 \qquad \gamma_y, \gamma_z \;=\; 0$$

Inserting these conditions into Eqs. (3.22) and defining γ_x as the constant thrust force per unit of mass to be applied over the time t, the equations of motion become

$$\begin{aligned} x(t) &= \frac{1}{\omega^2}\gamma_x \left(4(1-\cos(\omega t)) - \frac{3}{2}\omega^2 t^2\right) \\ z(t) &= \frac{2}{\omega^2}\gamma_x(\sin(\omega t) - \omega t) \end{aligned} \tag{3.59}$$

By differentiation one obtains the velocities

$$\begin{aligned} \dot{x}(t) &= \gamma_x \left(\frac{4}{\omega} \sin(\omega t) - 3t \right) \\ \dot{z}(t) &= \frac{2}{\omega} \gamma_x \left(\cos(\omega t) - 1 \right) \end{aligned} \tag{3.60}$$

Applications of tangential thrust manoeuvres with finite duration

Quasi-impulsive x-thrust manoeuvres The exact solution for the realistic case of thrust manoeuvres with limited thrust level and duration is given in appendix A, Eqs. (A.43)–(A.49). The position and velocities achieved after applying a constant thrust force per unit of mass γ_x, for time t, can easily be calculated, however, by using Eqs. (3.59) and (3.60). The total ΔV applied after time $t = \tau$ is, for a constant thrust level,

$$\Delta V = \gamma_x \tau$$

Further evolution of the trajectory can be obtained (using the simple tools provided in this chapter) by inserting the position and velocities achieved at the end of the thrust at time τ as initial conditions into Eqs. (3.22) and setting the forces $\gamma_x, \gamma_y, \gamma_z$ to zero, for the further free motion.

Example. Tangential transfer with finite boosts to a different orbit altitude (Hohmann transfer)

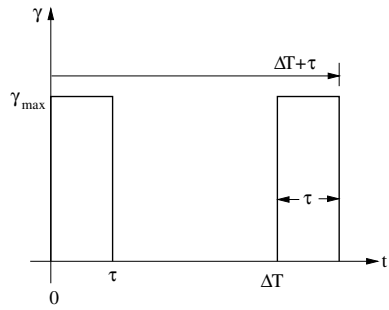

Figure 3.28. Two-boost transfer manoeuvres with finite pulse duration.

The manoeuvre starts at a distance $Z_0 = \Delta z$ from the target orbit. For an impulsive transfer, the necessary ΔV_x to achieve the desired change of altitude Δz is, according to Eq. (3.32),

$$\Delta V_x = \frac{\omega}{4} \Delta z$$

In order to achieve the same Δz in the case of a finite thrust transfer with a limited $\gamma_x = \gamma_{x-\max}$, the same $\Delta V_x = \gamma_x \tau$ must be applied (valid only for $\tau \ll \Delta T$). The necessary boost duration is then

$$\tau = \frac{\omega \Delta z}{4\gamma_x} \tag{3.61}$$

The interval from the start of the first to the start of the second tangential boost is still half an orbital revolution:

$$\Delta T = \frac{\pi}{\omega}$$

The equations of motion during the boost can be obtained from Eqs. (3.59) by inserting the chosen Z_0, τ and γ_x, γ_z. The equations of the free motion between the boosts are obtained by inserting the obtained results for $x(\tau)$, $\dot{x}(\tau)$ and $z(\tau)$, $\dot{z}(\tau)$ into the CW equations (3.22):

$$\begin{aligned} x(t) &= X_0 + \frac{3}{2}(\omega Z_0 - 2\gamma_x \tau)t + \frac{3}{2}\gamma_x \tau^2 + \frac{4}{\omega}\gamma_x \tau \sin\left(\omega\left(t - \frac{\tau}{2}\right)\right) \\ z(t) &= Z_0 - \frac{2}{\omega}\gamma_x \tau + \frac{2}{\omega}\gamma_x \tau \cos\left(\omega\left(t - \frac{\tau}{2}\right)\right) \end{aligned} \tag{3.62}$$

Continuous x-thrust transfer to a different altitude The following example is the extreme case of a continuous thrust over one entire orbital revolution. It shows that the most important difference between purely impulsive manoeuvres and constant thrust manoeuvres is the difference in duration. The change in orbital height, which can be achieved with a particular amount of ΔV, is the same.

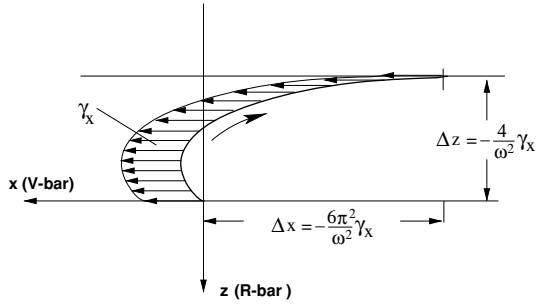

Figure 3.29. Continuous x-thrust transfer to different altitude.

The special case shown in figure 3.29, i.e. a transfer to a different orbital altitude by continuous thrust over one orbital revolution, can be of interest, either because of thrust level limitations or because of safety considerations (see section 4.1). For the transfer

time of one orbital period, $t = T$, $\omega t = 2\pi$, and for the general case of a trajectory starting at x_0, z_0, Eqs. (3.59) become

$$\begin{aligned} \Delta x = x_T - x_0 &= -\frac{6\pi^2}{\omega^2}\gamma_x \\ \Delta z = z_T - z_0 &= -\frac{4\pi}{\omega^2}\gamma_x \end{aligned} \tag{3.63}$$

and Eqs. (3.60) become

$$\begin{aligned} \dot{x_T} &= \frac{-6\pi}{\omega}\gamma_x \\ \dot{z_T} &= 0 \end{aligned} \tag{3.64}$$

The continuous thrust force per mass unit required over T to achieve the difference in altitude Δz is then

$$\gamma_x = \frac{-\omega^2}{4\pi}\Delta z \tag{3.65}$$

With Eq. (3.65) the total ΔV required is

$$|\Delta V_{\text{total}}| = |\gamma_x|\, T = \frac{\omega}{2}\Delta z$$

This is the same ΔV requirement as for the impulsive (Hohmann) transfer. The continuous thrust orbit raising manoeuvre is in its results indeed similar to the Hohmann transfer, except for a transfer duration of T instead of $T/2$ and for the progress in x-direction, which is double.

Transfer by continuous z-thrust

This case is similar to that for the x-thrust transfer, i.e. we are interested in limitation of thrust level and trajectory safety.

For the easiest case, with the trajectory starting in $\boldsymbol{O_{lo}}$, the initial conditions are

$$x_0, y_0, z_0 = 0 \qquad \dot{x_0}, \dot{y_0}, \dot{z_0} = 0 \qquad \gamma_x, \gamma_y = 0$$

Inserting the initial conditions into Eqs. (3.22) and defining γ_z as the constant thrust force to be applied, the equations of motion become

$$\begin{aligned} x(t) &= \frac{2}{\omega^2}\gamma_z(\omega t - \sin(\omega t)) \\ z(t) &= \frac{1}{\omega^2}\gamma_z(1 - \cos(\omega t)) \end{aligned} \tag{3.66}$$

By differentiation one obtains the velocities

$$\begin{aligned} \dot{x}(t) &= \frac{2}{\omega}\gamma_z\,(1-\cos(\omega t)) \\ \dot{z}(t) &= \frac{1}{\omega}\gamma_z\,\sin(\omega t) \end{aligned} \tag{3.67}$$

Applications of radial thrust manoeuvres with finite duration

Quasi-impulsive z-thrust manoeuvres In analogy to the case of continuous x-thrust transfer, Eqs. (3.66) and (3.67) can be used for the calculation of trajectory and velocity of a z-thrust manoeuvre with the boost duration $t = \tau$. The total ΔV is correspondingly

$$\Delta V = \gamma_z \tau$$

Example. Radial thrust transfer with finite boosts to a new x-position on V-bar

The radial boost starts at a position X_0 on the target orbit. For an impulsive transfer the necessary ΔV_z to achieve the desired change of x-position $\Delta x = X_\mathrm{F} - X_0$ is, according to Eq. (3.37),

$$\Delta V_z = \frac{\omega}{4}\Delta x$$

For a finite thrust transfer, the interval between the boosts is again half an orbital revolution. To achieve the same Δx with a limited $\gamma_z = \gamma_{z-\max}$ the necessary boost duration is (valid only for $\tau \ll \Delta T$, $\Delta T =$ time between the boosts)

$$\tau_z = \frac{\omega \Delta x}{4\gamma_z} \tag{3.68}$$

The equations of motion during the boost can be obtained from Eqs. (3.66) by inserting x_0, τ_z and γ_z. The equations of the free motion between the boosts are obtained by inserting the calculated results for $x(\tau_z)$, $\dot{x}(\tau_z)$ and $z(\tau_z)$, $\dot{z}(\tau_z)$ into the CW equations (3.22):

$$\begin{aligned} x(t) &= X_0 + \frac{2}{\omega}\gamma_z\ \tau_z \left[1 - \cos\left(\omega\left(t - \frac{\tau_z}{2}\right)\right)\right] \\ z(t) &= \frac{1}{\omega}\gamma_z\ \tau_z\ \sin\left(\omega\left(t - \frac{\tau_z}{2}\right)\right) \end{aligned} \tag{3.69}$$

If the transfer does not take place exactly on the target orbit, but at a distance Δz, the x-velocity according to Eq. (3.24), $\dot{x} = \frac{3}{2}\omega\,\Delta z$, has to be taken into account and must be compensated for by corresponding x-thrusts. The resulting equations of motion will then also include γ_x and τ_x terms. The duration of the additional boost in the x-direction is, according to Eq. (3.61), again

$$\tau_x = \frac{\omega \Delta z}{4\gamma_x}$$

The time interval between the boosts is (MATRA 1993)

$$\Delta T = \frac{\pi}{\omega} + \frac{2}{\omega}\arctan\left(\frac{4\Delta z}{\Delta x}\right) \tag{3.70}$$

The resulting free motion between the boosts is (MATRA 1993)

$$\begin{aligned} x(t) &= X_0 + 6\Delta z(\omega t - \sin(\omega t)) + \frac{\gamma_x}{\omega}\tau_x\left[4\sin\left(\omega\left(t-\frac{\tau_x}{2}\right)\right) - 3\omega\left(t-\frac{\tau_x}{2}\right)\right] + \cdots \\ &\quad + 2\frac{\gamma_z}{\omega}\tau_z\left[1-\cos\left(\omega\left(t-\frac{\tau_z}{2}\right)\right)\right] \\ z(t) &= \Delta z(4-3\cos\omega t) - 2\frac{\gamma_x}{\omega}\tau_x\left[1-\cos\left(\omega\left(t-\frac{\tau_x}{2}\right)\right)\right] + \frac{\gamma_z}{\omega}\tau_z\sin\left(\omega\left(t-\frac{\tau_z}{2}\right)\right) \end{aligned} \tag{3.71}$$

Continuous thrust transfer along V-bar The interest in the special case of a transfer along V-bar by continuous thrust (figure 3.30) is the same as in the previous case, i.e. thrust limitations and safety considerations. For the transfer time of one orbital period

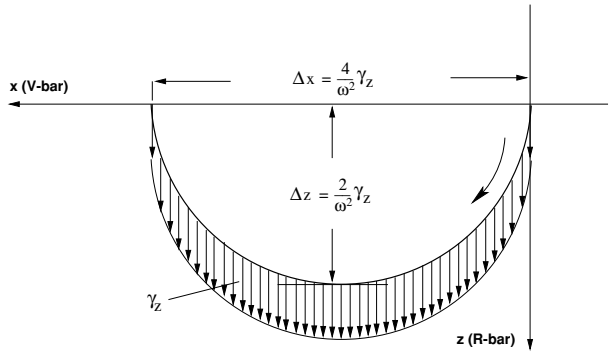

Figure 3.30. Transfer along V-bar by continuous z-thrust.

($t = T, \omega t = 2\pi$) and for the general case of a trajectory starting at x_0, z_0, Eqs. (3.66) become

$$\begin{aligned} \Delta x = x_T - x_0 &= \frac{4\pi}{\omega^2}\gamma_z \\ \Delta z = z_T - z_0 &= 0 \end{aligned} \tag{3.72}$$

The maximum extension of the trajectory in the z-direction is at $t = T/2$:

$$z_{T/2} = \frac{2}{\omega^2}\gamma_z \tag{3.73}$$

The continuous thrust required over T to achieve the intended Δx is, from Eqs. (3.72),

$$\gamma_z = \frac{\omega^2}{4\pi}\Delta x \tag{3.74}$$

This transfer along V-bar is similar to the radial impulse transfer, with a transfer time of T instead of $T/2$ and with continuous radial thrust along the arc. In contrast to the straight line V-bar transfer, there are no thrusts in the $+$ and $-x$-direction at the beginning and end of the transfer trajectory. The total ΔV is

$$\Delta V_{\text{total}} = \gamma_z T = \frac{\omega}{2}\Delta x$$

This is the same ΔV requirement as for the impulsive transfer along V-bar with radial impulses ΔV_z.

Continuous thrust in the *y*-direction

For reasons of completeness, the equations for a continuous constant thrust manoeuvre in the y-direction are given here. For a trajectory starting in $\boldsymbol{O_{lo}}$ the initial conditions are

$$x_0, y_0, z_0 = 0 \qquad \dot{x_0}, \dot{y_0}, \dot{z_0} = 0 \qquad \gamma_x, \gamma_z \;=\; 0$$

With these initial conditions and with γ_y defined as the continuous thrust force, Eqs. (3.22) become

$$\begin{aligned} x(t) &= 0 \\ y(t) &= \frac{1}{\omega^2}\gamma_y(1-\cos(\omega t)) \\ z(t) &= 0 \end{aligned} \tag{3.75}$$

By differentiation one obtains the velocity

$$\dot{y}(t) \;=\; \frac{1}{\omega}\gamma_y \sin(\omega t) \tag{3.76}$$

As in the case of continuous x- and z-thrust transfer, Eqs. (3.75) and (3.76) can be used for the calculation of trajectory and velocity of a y-thrust manoeuvre with the duration t_t. The ΔV cost is correspondingly

$$\Delta V = \gamma_y t_t$$

Forced motion circular fly-around

The forced motion circular fly-around can be of interest when a certain fly-around angle has to be reached and when the distance between chaser and target vehicles has to be kept constant because of safety or other reasons. Such a transfer trajectory can be used, e.g., when the docking axis has a small angle w.r.t. V-bar or when the fly-around has to be performed against the natural orbital motion, e.g. from $+$V-bar to $+$R-bar. For larger angles in the direction of orbital motion, e.g. for a 90 deg fly-around from $-$V-bar

to +R-bar, tangential or radial impulsive manoeuvres will be preferred because of the lower expenditure on ΔV. The following initial conditions are assumed:

$$\begin{array}{ll} x_0 = -R_{\rm fa} & \dot{x_0}, \dot{y_0} = 0 \\ y_0, z_0 = 0 & \dot{z_0} = \Delta V_{zi} \end{array} \qquad \gamma_y = 0$$

where $R_{\rm fa}$ is the fly-around radius. With $\dot{\alpha}$ being the angular rate of the fly-around, the equations of motion become, for the case shown in figure 3.31,

$$\begin{aligned} x(t) &= -R_{\rm fa}\cos(\dot{\alpha}t) \\ y(t) &= 0 \\ z(t) &= R_{\rm fa}\sin(\dot{\alpha}t) \end{aligned} \tag{3.77}$$

The initial ΔV that has to be applied is

$$\Delta V_{z\rm i} = R_{\rm fa}\dot{\alpha} \tag{3.78}$$

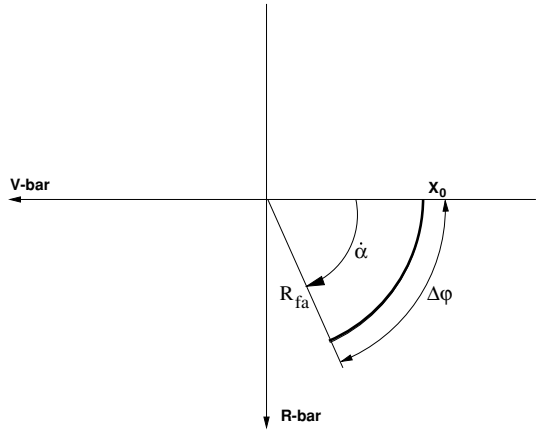

Figure 3.31. Forced motion circular fly-around.

The forces γ_x and γ_z that have to be applied over the arc can be obtained by inserting into Eqs. (3.21) the above initial conditions, the $x(t)$ and $z(t)$ positions from Eq. (3.77) and the velocities and accelerations obtained by differentiation of Eq. (3.77):

$$\begin{aligned} \gamma_x(t) &= -R_{\rm fa}\dot{\alpha}(2\omega - \dot{\alpha})\cos(\dot{\alpha}t) \\ \gamma_z(t) &= -R_{\rm fa}(\dot{\alpha}^2 - 2\omega\dot{\alpha} + 3\omega^2)\sin(\dot{\alpha}t) \end{aligned} \tag{3.79}$$

where ω is the angular rate of the orbit.

The final ΔVs that have to be applied in the x- and z-directions to stop the motion at the fly-around angle $\Delta\varphi = \dot{\alpha}t$ are

$$\begin{aligned} \Delta V_{x\rm f} &= R_{\rm fa}\dot{\alpha}\sin(\Delta\varphi) \\ \Delta V_{z\rm f} &= R_{\rm fa}\dot{\alpha}\cos(\Delta\varphi) \end{aligned} \tag{3.80}$$

The transfer time for a fly-around angle $\Delta\varphi$ is $\Delta t = t_1 - t_0 = \Delta\varphi/\dot{\alpha}$.

To the above final ΔVs must be added the velocities which the vehicle is intended to assume at the end of the fly-around, otherwise a motion as shown in figure 3.11 will commence. In the case of station keeping at this point, the continuous force per unit of mass of Eq. (3.55) for $z = R_{\mathrm{fa}} \sin(\Delta\varphi)$ has to be applied.

The ΔVs required during the transfer $\Delta\varphi$ are

$$\begin{aligned} \Delta V_{x\varphi} &= \int_{t_0}^{t_1} \gamma_x(t)\mathrm{d}t \\ \Delta V_{z\varphi} &= \int_{t_0}^{t_1} \gamma_z(t)\mathrm{d}t \end{aligned} \tag{3.81}$$

The total ΔV expenditure for a circular fly-around over an angle $\Delta\varphi$ is

$$\Delta V_{\mathrm{total}} = |\Delta V_{\mathrm{zi}}| + |\Delta V_{x\varphi}| + |\Delta V_{z\varphi}| + |\Delta V_{\mathrm{xf}}| + |\Delta V_{\mathrm{zf}}|$$

3.4 Final remark on the equations of motion

The intention of this chapter was to provide a sort of tool-kit for the calculation of properties of the most important types of trajectories and manoeuvres used in rendezvous approaches. Whereas all trajectories have been treated so far as undisturbed cases, in reality external disturbance forces and errors in the assumed initial conditions and applied ΔVs have to be taken into account. These are, in the first instance, not included in the equations derived here. However, in most cases:

- external disturbance forces can be treated as additional constant force components γ, at least over a particular time;
- thrust errors can be treated as additional x-, y-, z-components in the applied ΔV; and
- navigation errors can be treated as additional x-, y-, z-components in the initial conditions.

The disturbed trajectories can then be calculated, using the same set of equations as for the undisturbed ones, by simply adding the additional initial conditions and constant forces.

The most important equations of the undisturbed open loop trajectories are listed in Table 3.1, and examples for the combination of initial conditions and equations of motion are shown in the following sections. The sources and effects of trajectory deviations due to external disturbances and errors of the onboard system are addressed in sections 4.2 and 4.3 of the following chapter.

Table 3.1. Equations of motion.

Type of manoeuvre and equation numbers	Initial conditions	Equations of motion
Impuls. change V_x (3.28)	$\boldsymbol{O}_{\mathbf{lo}}$, ΔV_x, $t = 0$	$x(t) = \frac{1}{\omega}\Delta V_x(4\sin(\omega t) - 3\omega t)$ $z(t) = \frac{2}{\omega}\Delta V_x(\cos(\omega t) - 1)$
Impuls. change V_y (3.40)	$\boldsymbol{O}_{\mathbf{lo}}$, ΔV_y, $t = 0$	$y(t) = \frac{1}{\omega}\Delta V_y \sin(\omega t)$
Impuls. change V_z (3.34)	$\boldsymbol{O}_{\mathbf{lo}}$, ΔV_z, $t = 0$	$x(t) = \frac{2}{\omega}\Delta V_z(1 - \cos(\omega t))$ $z(t) = \frac{1}{\omega}\Delta V_z \sin(\omega t)$
Contin. force, x-dir. (3.59)	$\boldsymbol{O}_{\mathbf{lo}}$, γ_x, $t = 0$	$x(t) = \frac{1}{\omega^2}\gamma_x\,(4(1 - \cos(\omega t))$ $-\frac{3}{2}\omega^2 t^2)$ $z(t) = \frac{2}{\omega^2}\gamma_x(\sin(\omega t) - \omega t)$
Contin. force, y-dir. (3.75)	$\boldsymbol{O}_{\mathbf{lo}}$, γ_y, $t = 0$	$y(t) = \frac{1}{\omega^2}\gamma_y(1 - \cos(\omega t))$
Contin. force, z-dir. (3.66)	$\boldsymbol{O}_{\mathbf{lo}}$, γ_z, $t = 0$	$x(t) = \frac{2}{\omega^2}\gamma_z(\omega t - \sin(\omega t))$ $z(t) = \frac{1}{\omega^2}\gamma_z(1 - \cos(\omega t))$
Straight line V-bar (3.44), (3.45)	$\boldsymbol{O}_{\mathbf{lo}}$, ΔV_{x0}, $t = 0$	$x(t) = \Delta V_x t$, $\gamma_z = 2\omega\Delta V_x$
Straight line R-bar (3.49), (3.50)	$\boldsymbol{O}_{\mathbf{lo}}$, ΔV_{z0}, $t = 0$	$z(t) = \Delta V_z t$ $\gamma_x = -2\omega\Delta V_z$ $\gamma_z = -3\omega^2\Delta V_z t$
Circular fly-around (3.77), (3.79)	$x = -R_{fa}$, $t = 0$ $\dot{z}_0 = \Delta V_{z0}$	$x(t) = -R_{fa}\cos(\dot{\alpha}t)$ $z(t) = R_{fa}\sin(\dot{\alpha}t)$ $\gamma_x(t) = -R_{fa}\dot{\alpha}(2\omega - \dot{\alpha})\cos(\dot{\alpha}t)$ $\gamma_z(t) = -R_{fa}(\dot{\alpha}^2 - 2\omega\dot{\alpha}$ $+3\omega^2)\sin(\dot{\alpha}t)$
Hold point at z_0 (3.55)	$x_0 = 0, \dot{x}_0 = 0, t = 0$ $z_0 = Z_0$	$x(t), y(t) = 0$ $z(t) = Z_0$, $\gamma_z = -3\omega^2 Z_0$
Hold point at y_0 (3.58)	$x_0 = 0, \dot{x}_0 = 0, t = 0$ $y_0 = Y_0$	$x(t), z(t) = 0$ $y(t) = Y_0$, $\gamma_y = \omega^2 Y_0$

Table 3.1. (*continued*). Equations of motion.

Type of manoeuvre and equation numbers	Initial conditions	Equations of motion
Free drift, start at z_0 on circular orbit (3.25)	$x_0 = 0, \dot{x}_0 = \frac{3}{2}\omega Z_0$ $z_0 = Z_0, t = 0$	$x(t) = \frac{3}{2}\omega Z_0 t$ $z(t) = Z_0$
Free drift, release at Z_0 with velocity of target (3.26)	$x_0 = 0, \dot{x}_0 = 0, t = 0$ $z_0 = Z_0, \dot{z}_0 = 0$	$x(t) = 6Z_0(\omega t - \sin(\omega t))$ $z(t) = Z_0(4 - 3\cos(\omega t))$
Free drift, start at y_0	$y_0 = Y_0, \dot{y}_0 = 0, t = 0$	$y(t) = Y_0 \cos(\omega t)$
Free drift, start at x_0 (3.27)	$x_0 = X_0, \dot{x}_0 = 0, t = 0$	$x(t) = X_0$

3.4.1 Examples for combined cases

Combined cases can be obtained by adding, where applicable, the equations of motion and the initial conditions belonging to each single manoeuvre.

Example 1

To obtain a trajectory with continuous force in the x-direction starting at $x_0 = X_0$ and $z_0 = Z_0$ on a lower orbit, we add initial conditions and equations of motion of the following cases (see Table 3.1):

(1) 'contin. force, x-dir.',

(2) 'free drift, start at x_0',

(3) 'free drift, start at z_0 on circular orbit'.

The results are as follows. For combined initial conditions $(1) + (2) + (3)$

$$\begin{array}{lllllllll} x_0 & = & 0 + X_0 + 0 & \quad \dot{x}_0 & = & 0 + 0 + \frac{3}{2}\omega Z_0 & \quad \gamma_x & = & \gamma_x + 0 + 0 \\ y_0 & = & 0 + 0 + 0 & \quad \dot{y}_0 & = & 0 & \quad \gamma_y & = & 0 \\ z_0 & = & 0 + 0 + Z_0 & \quad \dot{z}_0 & = & 0 & \quad \gamma_z & = & 0 \end{array}$$

For combined equations of motion $(1)+(2)+(3)$

$$\begin{aligned} x(t) &= \gamma_x \left(\frac{4}{\omega^2}(1-\cos(\omega t)) - \frac{3}{2}t^2 \right) + X_0 + \frac{3}{2}Z_0\omega t \\ z(t) &= \frac{2}{\omega^2}\gamma_x(\sin(\omega t) - \omega t) + 0 + Z_0 \end{aligned}$$

Example 2

To obtain a forced motion R-bar trajectory starting at $x_0 = X_0$ and $z_0 = Z_0$ with $\dot{x}_0 = 0$ we add initial conditions and equations of motion of the following cases:

(1) 'straight line R-bar',

(2) 'hold point at x_0' = 'free drift, start at x_0',

(3) 'hold point at z_0'.

The results are as follows. For combined initial conditions $(1)+(2)+(3)$

$$\begin{aligned} x_0 &= 0 + X_0 + 0 & \dot{x}_0 &= 0 + 0 + 0 \\ y_0 &= 0 + 0 + 0 & \dot{y}_0 &= 0 \\ z_0 &= 0 + 0 + Z_0 & \dot{z}_0 &= \Delta V_z + 0 \end{aligned}$$

For combined equations of motion $(1)+(2)+(3)$

$$\begin{aligned} x(t) &= 0 + x_0 + 0 & \gamma_x &= -2\omega\Delta V_z \\ z(t) &= \Delta V_z t + 0 + z_0 & \gamma_z &= -3\omega^2\Delta V_z t - 3\omega^2 z_0 \end{aligned}$$